Kansas Geological Survey

Technical Series 22

Mineralogical and Chemical Evolution of Lamproites in Woodson and Wilson Counties, Southeastern Kansas

Robert L. Cullers and Pieter Berendsen

Lawrence, KS
2011

Editor: Marla Adkins–Heljeson
Graphic Designer: Jennifer Sims

Contents

The Mineralogical and Chemical Evolution of Lamproites in Woodson and Wilson Counties, Southeaster Kansas 1
  Abstract 1
  Experimental 1
  Geology 2
    Mineralogy 2
      General Mineralogy 2
      Mineral Compositions 2
  Elemental Compositions 2
    Composition Compared to Other Lamproites 2
    Comparison of the Composition of the Rose and the Silver City Dome Lamproite 3
    Internal Variation of Composition within the Silver City Cores 3
    Internal Variation of Composition within the Rose Dome Cores 9
    Elemental Trends vs. Mg# 9
  Discussion 31
    Formation of the Primary Magmas 31
    Internal Variation within the Sills 34
References 35

Tables

1—A comparison of X-ray fluorescence values and ICP-MS values of BIR-1 with one another and with those of others. . . .3
2—Mineral compositions of the lamproites 5
3—The composition of lamproites and associated sedimentary rocks of Woodson County 10
4—The means and standard deviations of lamproite samples in southeastern Kansas 26
5—Averages of lamproites compared to other lamproites. 32

Figures

1—Location study area and of cores used in this study. 2
2—The cationic Al and Ti compositions of clinopyroxenes from cores 92-5 and 92-11 of the Silver City Dome are compared to those of West Kimberly, Smoky BUtte, Leucite Hills, Prairie Creek, and southeastern Spain 4
3—The composition of Na_2O (weight percent) and FeO (weight percent) of 92-5 and 92-11 are compared to other lamproites 4
4—The cationic Ti and Na/K ratios of amphiboles from cores 92-5 and 92-11 are compared to other lamproites 7
5—The Al_2O_3 and FeO compositions (weight percent) of micas from cores 92-5 and 92-11 (Silver City Dome) and Eagle 4 (Rose Dome) are compared to other lamproites 8
6—The Al_2O_3 and TiO_2 composition (weight percent) of micas from cores 92-5, 92-11, and Eagle 4 are compared to other lamproites. 8
7—The composition of CaO in all samples is plotted against Al_2O_3. 8
8—Concentration of the average values of the Silver City and Rose Dome lamproites are normalized to primitive mantle 9
9—The change of TiO_2 concentration of the shallow cores of the Silver City Dome with depth 29
10—The change of MgO concentration of the shallow cores of the Silver City Dome with depth 30
11—The change is SiO2 concentration of the shallow Silver City Dome samples with depth. 31
12—The correlation of CaO and P_2O_5 in the shallow Silver City Dome and the Rose Dome 34
13—The change of TiO_2 concentration of the shallow cores of the deeper Eagle cores of the Rose Dome with depth. 35
14—The change of MgO concentration of the deeper Eagle cores of the Rose Dome with depth. 35
15—The change of SiO_2, Al_2O_3, K_2O, and P_2O_5 with Mg# of the deeper Eagle cores of the Rose Dome and the shallow Silver City Dome 36
16—The change of LO1, Ni, Co, and Cr with Mg# of the deeper Eagle cores of the Rose Dome and the shallow Silver City Dome 37

Mineralogical and Chemical Evolution of Lamproites in Woodson and Wilson Counties, Southeastern Kansas

Robert L. Cullers[1] and Pieter Berendsen[2]

[1]Department of Geology, Thompson Hall, Kansas State University, Manhattan, KS 66506
[2]Kansas Geological Survey (retired), Lawrence, KS 66047

Abstract

The major and trace element content of 123 lamproites and associated sedimentary rock samples from six cores of the Silver City Dome and two cores from the Rose Dome in southeastern Kansas were analyzed. The lamproites are ultrapotassic (weight percent K_2O/Na_2O = 2.0 to 22.1), alkalic (molecular $[K_2O + Na_2O]/Al_2O_3$ = 1.01 to 3.04), and are enriched in mantle-incompatible elements (e.g., light REE, Ta, Hf, Ba, Rb, Sr, Th). The low Al_2O_3 content of these samples is consistent with lamproites formed in stable continental settings such as those from West Kimberley, Australia, and Smoky Butte, Montana. Also the lack of a significant negative Ta and Nb anomaly in mantle-normalized plots precludes the source rocks having been involved in subduction.

The samples from the Silver City cores are composed of mostly serpentinized olivine and mica with lesser amounts of K-richterite, diopside, rutile, apatite, perovskite, and spinel in a serpentinized groundmass. The Rose Dome cores contain mostly serpentinized olivine and mica with minor diopside, spinel, perovskite (more abundant than at Rose Dome), xenotime, and feldspar. Most mica compositions follow the trend of decreasing FeO and Al_2O_3 similar to trends of the Guess Core and the Wolgidite trend at West Kimberly. Micas enriched in Ba and Ti (BaO = 16.6–19.3 weight percent; TiO_2 = 26.0– 27.8 weight percent) rim some micas of more normal composition. These very high Ba and Ti-rich micas have not been found in other lamproites or other types of alkalic rocks.

The average composition of the shallow cores at the Silver City Dome are similar to one another (except for Na_2O, Li, and Cs), although the average composition of the shallow cores are different than the previously studied deeper Guess and Ecco Ranch cores in this area. The average composition of the two Eagle cores at Rose Dome are similar to one another, but they are higher in Fe_2O_3 (total), MgO, CaO, P_2O_5, Th, Co, Ni, Cr, U, Y, REE, Cu, and Cs concentrations than the shallow cores from the Silver City Dome.

Metasomatized mantle (lherzolite-harzburgite) containing varied amounts of veins containing clinopyroxene, K-Ti amphibole, phlogopite, apatite, and K-Ba-Zr-Nb titanates could have melted in varied amounts to form the lamproites. The lower SiO_2 and Al_2O_3 and higher MgO lamproites at Rose Dome likely result from melting at a higher temperature of more lherzolite-harzburgite and less vein material than the more SiO_2-rich and MgO-poor lamproites at Silver City.

Also the concentration of most elements varies vertically in the cores, and the variation in the elemental concentration can be related to mineral gravity settling, flow differentiation, or volatile transport processes within the sills. For example, at the Silver City Dome, concentrations of olivine and phlogopite can be related to the samples with the lowest SiO_2 and highest MgO, Mg#, Ni, and Co content. The portions of the cores with the highest concentrations of K_2O, Al_2O_3, and Sc may be correlated to samples with the highest phlogopite. Also Ba often decreases in amount upward in many cores at the Silver City Dome and is enriched in overlying hornfels compared to the unaltered overlying shale. Ba movement in H_2O-rich fluids into the overlying hornfels can explain this observation. Curiously, overlying limestones are not enriched in Ba, so at least locally the limestones may be impervious to the fluids.

Experimental

The major elements and trace elements were analyzed by X-ray fluorescence (XRF) and inductively coupled plasma mass spectrometry (ICP-MS) at the SRS Company in Toronto, Canada. One to 15 grams of each sample (pre-dried at 105°C for about 8 hours) were dissolved in aqua regia in a 80°C–90°C water bath and were diluted as needed for ICP-MS analyses. The diluted samples were analyzed on either an Elan 6100 or PQ3 mass spectrometer. An in-house reference standard was analyzed every 48th sample, and duplicates were analyzed every 12th sample. Results of the U.S. Geological Survey standard basalt, BIR-1, are given in table 1 along with average values from other sources (Govindaraju, 1994).

The pre-dried samples were also analyzed using XRF. Two grams of each sample were heated in an oxygen-purged furnace at 950°C for 1 hour. The samples were mixed with 7.7 grams of a 50/50 mix of lithium tetraborate and lithium metaborate and fused in an automatic fluxer. The melt was poured into a platinum mold to form a 40-mm glass disk. Loss on ignition (LOI) was obtained from the weight loss on heating at 950°C as described above. The glass disks were analyzed on an automated Siemens SRS–3000 X-ray fluorescence spectrometer that was calibrated using 41 different rocks. Duplicates of samples were analyzed every 20th sample, and a house control sample was analyzed every 55th sample. Results of the BIR-1 using XRF are also given in table 1. Results of the SRS analyses on BIR-1 generally agreed with the averages of other analysts.

Also a number of samples were rechecked using ICP-MS at the University of Kansas using similar techniques as those of the SRS. Most results agreed well between labs and by different techniques, so the results on the same sample were averaged.

Geology

The geology of the lamproites and associated sedimentary rocks is described in Berendsen (2011). The location of the cores used in this study are shown in fig. 1 and also given in Berendsen (2011).

Mineralogy

General Mineralogy

The mineralogy of the lamproites at the surface at the Silver City Dome are porphyritic with megacrysts of mostly serpentinized olivine and mica with lesser diopside, chrome spinel, and richterite (Franks et al., 1971; Cullers et al., 1985; Coopersmith and Mitchell 1989). The groundmass is mostly serpentine.

The deeper Guess Core (305–312 m [1,000–1,023 ft] depth) and Ecco Ranch Core (237.5–247.5 m [779–812 ft] depth) at Silver City Dome are fine to coarse grained with usually little groundmass (Cullers et al., 1996). The main minerals in the Guess Core are mica and sanidine with lesser richterite, diopside, Ca-Si zeolite, apatite, shcherbakovite, wadeite, and perovskite. The main minerals in the Ecco Ranch Core are mica, sanidine, and richterite with lesser diopside, Ca-Si zeolite, and sphene. This sill is enriched in sanidine and depleted in mica and richterite in the mid to lower portions of the sill relative to the upper portion of the sill.

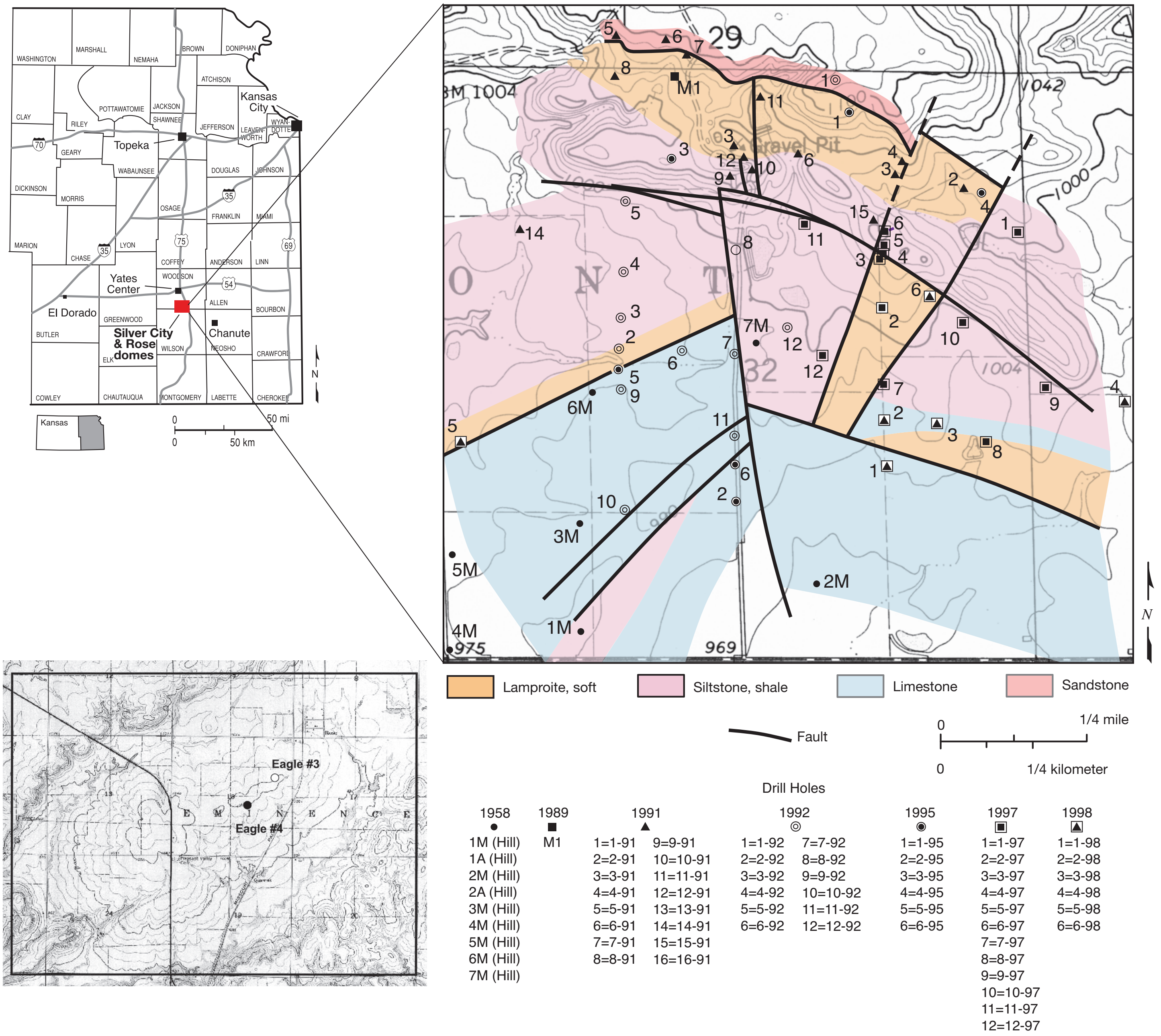

FIGURE 1—Location study area and of cores used in this study (Silver City dome to right and Rose dome to lower left).

The mineralogy of the shallow cores (92, 97, and 98 series) at the Silver City Dome is similar to that of the previously studied surface samples. Thus, the cores are composed of mostly serpentinized olivine and mica with lesser amounts of K-richterite, diopside, rutile, apatite, perovskite, and spinel in a serpentinized groundmass. Coarser crystals of especially serpentinized olivine, and to a lesser extent, mica, richterite, and diopside, are concentrated toward the center to lower center portions of the cores.

In contrast, cores at the Rose Dome contain somewhat different mineralogy compared to those at the Silver City Dome. For example, Eagle 4, like the shallow Silver City Dome cores, contains mostly serpentinized olivine and mica with minor diopside, spinel, and perovskite. The amount of perovskite, however, is often much more abundant in the Rose Dome cores (up to 5%) than the Silver City Dome cores (less than 1%). In addition, the Silver City Dome cores also may contain minor xenotime and feldspar.

Mineral Compositions

A few of the mineral compositions of representative samples of the lamproites also have been analyzed. The clinopyroxenes from the shallow Silver City cores are diopside with fairly low concentrations of Al_2O_3, FeO, Na_2O, and TiO_2 (table 2). The clinopyroxene compositions are similar to those of the deeper cores at the Silver City Dome and to those of West Kimberly (fig. 2).

The composition of the amphiboles of the shallow Silver City Dome cores are similar to those of the Guess core of the Silver City Dome, Smoky Butte, and West Kimberly although several samples fall outside these boundaries (fig. 3). Also the Ti concentrations are similar to those of West Kimberley (fig. 4). These amphiboles do not have the low Ti concentrations of those in the Guess and Silver City cores.

Most of the micas from the Silver City Dome and Eagle 4 cores follow trends of decreasing FeO and Al_2O_3 similar to trends of the Guess Core and the Wolgidite trend at West Kimberly (fig. 5). The Ba and Ti-enriched micas rimming micas of more normal composition of core 92–5 contain very low Al_2O_3 and FeO contents (fig. 5, table 2). Such high Ba and Ti-rich micas have not been found in other lamproites or other types of alkalic rocks (Mitchell and Bergman, 1991). The mica TiO_2 vs. the Al_2O_3 contents in the 92 and Eagle 4 cores follow the trend of decreasing Al_2O_3 at fairly constant TiO_2 similar to the Guess Core (fig. 6). These trends appear to be unique for Kansas lamproites.

Elemental Compositions

Composition Compared to Other Lamproites

The values of the elemental concentrations in the lamproites and associated sedimentary rocks are given in table 3. The averages and standard deviations of values of each core are given in table 4 (Cullers et al., 1985; Cullers et al., 1996); the averages and standard deviations of values at the Rose Dome and the Silver City Dome are given with similar values for other lamproites in table 5 (Jaques et al., 1984; Jaques et al., 1989; Toscani and Slavioli–Mariani, 2000; Chalapathi Rao et al., 2004).

The Kansas lamproites, like lamproites elsewhere, are ultrapotassic (weight percent $K_2O/Na_2O = 2.0$ to 22.1), alkalic (molecular $[K_2O + Na_2O]/Al_2O_3 = 1.01$ to 3.04), and are enriched in mantle-incompatible elements (light REE, Ta, Hf, Ba, Rb, Sr, Th; tables 3, 4, and 5). Most samples plot in the Group I region of CaO-Al_2O_3 plots due to their low CaO and Al_2O_3 content (fig. 7). The composition of these lamproites is thus consistent with the composition of lamproites formed in continental settings as would be expected from their location. The low Al_2O_3 content (<11.5%) of these samples are also consistent with lamproites forming in stable continental settings (e.g., West Kimberly, Australia; Leucite Hills, Wyoming; Smoky Butte, Montana) (Altherr et al., 2004). Samples with higher and more variable Al_2O_3 (up to 14.8%) form in active orogenic areas (e.g., Corsica, Spain, Alps) (Altherr et al., 2004).

The averages of the elemental concentrations from Cs (on the left) through Sm (to the right) of the Rose Dome and Silver City Dome are greater than 40 times the primitive mantle values (fig. 8). The normalized primitive mantle values of Ba and Pb are anomalously enriched relative to adjacent elements. The normalized mantle values of Ta and Nb are not as depleted relative to adjacent elements as is observed in some lamproites (Mitchell and Bergman, 1991; Altherr et al., 2004). Depletion of Ta and Nb have been related to subduction processes or to a Ti-rich mineral in the source holding back Ta and Nb (Mitchell and Bergman, 1991). Evidently such processes did not occur for these lamproites to significantly affect Ta and Nb. Negative Ti anomalies, however, are observed in these lamproites so potentially a Ti-rich mineral may have been present in the source to reduce the Ti in the melt. Ba might be anomalously enriched in the metasomatized source for these lamproites. The chondrite-normalized REE plots are enriched in the LREE relative to the HREE as is generally observed in lamproites (table 3). There are no Eu anomalies.

Comparison of the Composition of the Rose and the Silver City Dome Lamproites

The average values of most elements in the shallow cores at the Silver City Dome are similar to one another (table 4). The exceptions are Na_2O, Li, and Cs. Samples from the deeper Guess and Ecco Ranch cores at the Silver City Dome (Cullers et al., 1996) are higher in SiO_2 (not the Guess core), Al_2O_3 (not the Guess core), TiO_2 (not the Ecco Ranch core), total Fe_2O_3 (not the Ecco Ranch core), K_2O, Rb, Th (not the Ecco Ranch core), Hf, Zr, Y, and LREE, and lower in MgO and Mg# than the shallower cores at the Silver City Dome (table 5).

The Eagle cores at the Rose Dome are very similar in average concentrations to one another, but they contain different concentrations of many elements compared to those at the Silver City Dome (table 4). The averages of the Eagle cores are most notably lower in concentration of SiO_2, TiO_2, Al_2O_3, Na_2O, K_2O, Hf, and Li and higher in total Fe_2O_3, MgO, P_2O_5, Th, Co, Ni, Cr, U, Y REE, Cu, and Cs than averages of most of the shallower cores at the Silver City Dome (tables 4 and 5).

TABLE 1—A comparison of X-ray fluorescence values and ICP-MS values of BIR-1 with one another and with those of others.

	X-ray Fluorescence	**ICP-MS**	**USGS Certified Values[1] Mean (St.Dev.)**	**Geostandards Newsletter[2]**	**ICP-MS[3]**
SiO_2	47.7		47.96 (0.19)	47.77	
TiO_2	0.99	0.96	0.96 (0.01)	0.96	
$Al2O_3$	15.3	15.5	15.5 (0.15)	15.35	
Fe_2O_3(total)	11.5	11.0	11.3 (0.12)	11.26	
MnO	0.17	0.17	0.175 (.003)	0.17	
MgO	9.81	9.41	9.70 (0.079)	9.68	
CaO	12.9	12.9	13.3 (0.12)	13.2	
Na_2O	1.77		1.82 (0.05)	1.74	
K_2O		0.024	0.030 (0.003)	0.027	
P_2O_5	0.02	0.01	0.021 (0.001)		
LOI	0.01				
Rb		0.3		0.25	0.32
Ba		12	7	7	9.7
Sr	136	105	110 (2)	108	94.2
Th		0.05		0.03	0.04
Hf		<1	0.6 (0.08)	0.6	0.61
Zr	20	15	18 (1)	15.5	13.8
Ta		<0.5		0.04	
Co		55.9	52 (2)	51.4	54.2
Sc		39	44 (1)	44	41
Ni		168	170 (6)	166	174
Cr		374	370 (8)	382	399
U		<0.05		0.01	<0.03
Y	13	16.1	16 (1)	16	14.4
Nb	<2	3		0.6	2.11
La		0.66	0.63 (0.07)	0.62	0.61
Ce		2.0	1.9 (0.4)	1.95	1.85
Pr		0.41		0.37	0.36
Nd		2.6	2.5 (0.7)	2.5	2.21
Sm		1.1	1.1	1.1	1.06
Eu		0.54	0.55 (0.05)	0.54	0.49
Gd		1.9	1.8 (0.4)	1.85	1.63
Tb		0.36		0.36	0.33
Dy		2.6	4 (1)	2.5	2.33
Ho		0.6		0.57	0.52
Er		1.79		1.7	1.54
Tm		0.26		0.26	0.22
Yb		1.7	1.7 (0.1)	1.65	1.52
Lu		0.25	0.26	0.26	0.23
Cu		126	125 (4)	126	126
Li		<10	3.6 (0.2)	3.4	3.3
Zn		65	70 (9)	71	80.6
Cs		<.1		0.005	0.04
Ga		14	16	16	15.2
Ge		2		1.5	
Pb		<5	3	3	3.08
V		294	310 (11)	313	

1—USGS certified values are the March 1998 values by David B. Smith, USGS website—http://minerals.cr.usgs.gov/geo_chem_stand/icelandic.html

Numbers without a standard deviation are information values.

2—Govindaraju, K., 1994

3—Garbe–Schonberg and McMurtry, 1994

Internal Variation of Composition within the Silver City Cores

Some elements tend to vary in a similar way vertically in different shallow cores at the Silver City Dome. For example, CaO, TiO_2 (except core 92–5), Al_2O_3, K_2O, and CaO (except core 92–5) tend to be the lowest in the middle of each core and are the highest at the top and bottom of each core (e.g., see examples and exceptions in fig. 9). Also MgO, Mg#, Ni, and Co tend to be the highest toward the middle of each core, and they are the lowest at the top and bottom of each core (e.g., fig. 10). The concentrations of MgO, Mg#, Ni, and Co may be correlated to the amount of olivine and to a lesser extent to phlogopite, and the concentrations of Al_2O_3, K_2O, and Sc may be correlated to the amount of phlogopite (Mitchell, 1985; Mitchell and Bergman, 1991; Cullers et al., 1996). The amount of TiO_2 likely depends on the amount of perovskite or possibly shcherbakovite (Mitchell, 1985; Cullers et al., 1996). The TiO_2 content tends to correlate with the REE and Nb content in cores 92–11, 92–10, 97–10, and 97–11, suggesting the REE and Nb content also concentrate in perovskite as observed elsewhere (Mitchell and Bergman 1991). There is little correlation between Ba and TiO_2, suggesting that shcherbakovite is not a major Ba- and Ti-bearing mineral in these rocks.

Other elements do not have the same trend in variability with depth in different cores. For instance, the concentration of SiO_2 is the lowest in the middle of cores 92–5, 92–11, and 97–10, and tends to be the highest at the top and bottom of these cores (fig. 11). The lowest SiO_2 correlates to the highest amount of olivine (serpentine) and phlogopite (the most abundant minerals with the lowest SiO_2 content), and the highest SiO_2 content to the most diopside and K-richterite. In contrast, the amount of SiO_2 tends to decrease downward in core 92–10, suggesting that the amount of the lower SiO_2 minerals, olivine and phlogopite, systematically increase downward relative to the higher SiO_2 minerals. Also samples within core 92–10 are highest toward the base in MgO, Mg#, Ni, and Co, also consistent with this observation. Core 98–2 has about the same SiO_2 values through the core except for one low value in the middle. The SiO_2 in core 97–11 changes rather erratically through the core, but it has higher SiO_2 values toward the top. Again lower SiO_2 values correlate to the most olivine and phlogopite and the least to the minerals with higher SiO_2.

Variation in CaO might likely be correlated with diopside, richterite, or apatite variation in these rocks (Mitchell, 1985). If apatite is a major carrier of Ca, then there should be a correlation of CaO with P_2O_5. Indeed, CaO and P_2O_5 are correlated in cores 92–10, 98–2, 97–10, and 97–11 at a P_2O_5 of greater than about 0.8% (fig. 12), suggesting that apatite is a major carrier of these elements at higher CaO and P_2O_5 contents. The CaO and P_2O_5 are less correlated in the other cores. Samples with a poor correlation of CaO and P_2O_5 likely have more CaO incorporated in richterite or diopside. The Na_2O content changes differently with depth in different cores. The Na_2O is most likely concentrated in perovskite, shcherbakovite, or K-richterite (Mitchell, 1985; Cullers et al., 1996). The poor correlation of TiO_2 and Na_2O suggest that perovskite and shcherbakovite do not control most of the Na_2O. Instead, this suggests that K-richterite is a major control.

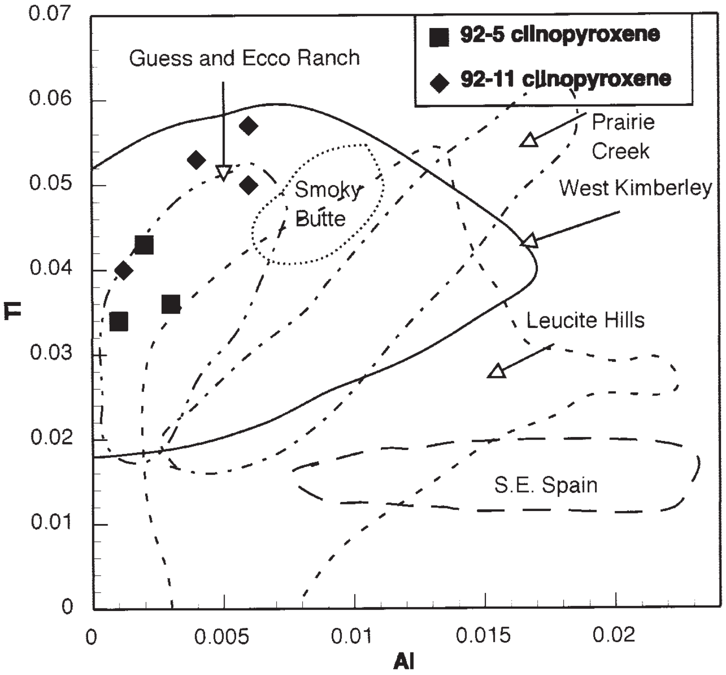

FIGURE 2— The cationic Al and Ti compositions of clinopyroxenes from cores 92-5 and 92-11 of the Silver City Dome are compared to those of West Kimberly, Smoky Butte, Leucite Hills, Prairie Creek (Arkansas), and southeastern Spain (Mitchell and Bergman 1991).

The loss on ignition (LOI) increases upward in cores 92–5, 92–11, 92–10, and 97–10. This suggests that the volatiles or hydrous minerals may have migrated upward to the top of these cores forming more minerals like serpentine, phlogopite, or richterite. The lack of any clear-cut trend in LOI with depth in cores 98–2 and 97–11 suggests that volatile migration may have not been so important.

The concentration of Ba decreases upward in cores 92–5, 92–10, 97–11, and the previous near-surface samples (Cullers et al., 1985). In the original study of one shallow core at the Silver City Dome, the concentration of Ba was also quite high in the overlying metamorphosed shales compared to the unmetamorphosed shales (Cullers et al., 1985). Thus, some of the Ba was believed to have moved out of the sill into the overlying bedrock. This could explain the decreased Ba upward within the sills if it is assumed that the decreased Ba flowed in H_2O-rich fluids upward into the overlying bedrock. Bedrock was sampled in this study above the sills in four of the cores. The amount of Ba was not higher in the overlying limestones next to the lamproite compared to those further away in core 92–5, but Ba was higher in cores 92–10 and 92–11 (table 4). The amount of Ba was incredibly high in a hornfels (greater than 15,000 ppm) above lamproite in core 97–11. Perhaps limestones provide a greater barrier to fluid migration and Ba transport than the shales. This conclusion is consistent with the cores 92–5, 92–10, and 97–11, and the previous near-surface samples all containing shale above them in which the Ba was reduced upward into the lamproite. None of the cores with limestone above them contained reduced Ba upward in the sill.

There is a good correlation of the Th and REE concentrations, and to a lesser extent, Th and the REE with Nb and U, suggesting that these elements are concentrated in the same minerals. These elements have been known to concentrate in perovskite (Mitchell and Bergman, 1991). In addition, Th may concentrate in priderite and apatite, REE in the Ca silicates, Nb in priderite, and U in apatite (Mitchell and Bergman, 1991). Moderate correlations of Th, La, Nb, and U with TiO_2 (enriched in perovskite and priderite) and P_2O_5 (enriched in apatite) are consistent with this possibility.

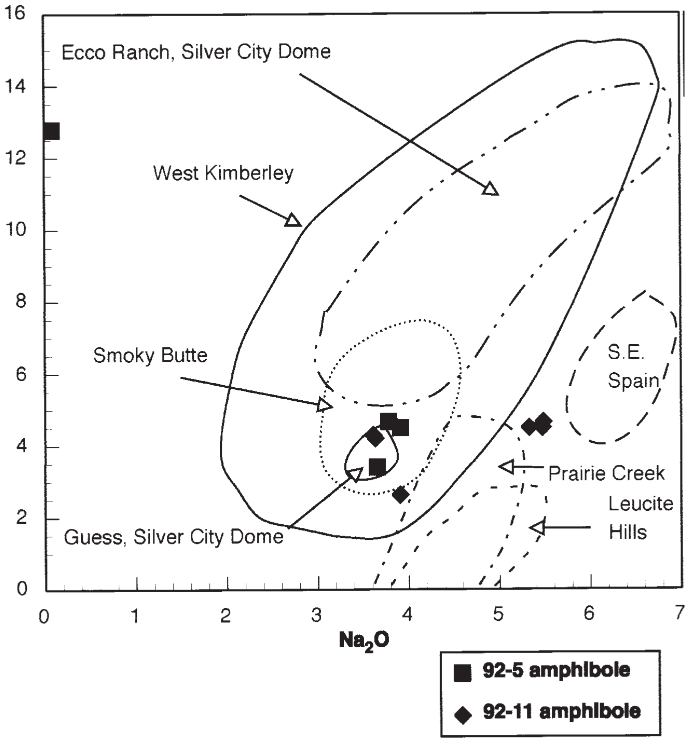

FIGURE 3—The composition of Na_2O (weight percent) and FeO (weight percent) of 92-5 and 92-11 are compared to other lamproites (Mitchell and Bergman 1991).

Finally Zr and Hf are well correlated with one another, suggesting that the same mineral controls them. These elements concentrate in the Zr-rich mineral, wadeite, and to a lesser extent, priderite, perovskite, and other Ti silicate minerals (Mitchell and Bergman, 1991).

Internal Variation of Composition within the Rose Dome Cores

The elemental changes of the two deeper Eagle cores at Rose Dome do not vary with depth like those of the shallow cores at the Silver City Dome. For instance, TiO_2, Al_2O_3, CaO, K_2O (not Eagle 4–22), P_2O_5, Rb (not Eagle 4–22), Sr, Zr, Y, Nb, REE, Ta, Sc, U, Cu, Zn (not Eagle 4–22), and Ga tend to decrease with increasing depth (see examples, fig. 14). The MgO, Mg#, Co, and Ni concentrations increase with increasing depth (see examples, fig. 14). This suggests that less phlogopite (correlates to K, Rb, Al, Sc, Zn, Cu), perovskite (correlates to Ti, Sr, Nb, REE, Y, Th, U), apatite (correlates to Ca, P, U), ilmenite (correlates to Ti), and wadeite (correlates to Zr and Hf), and more olivine (correlates to Mg, Mg#, Ni, Co) occurs in deeper portions than in shallower portions of these sills.

Also the concentration of SiO_2, Na_2O, and Ba (more variable in Eagle 4–22) tend to decrease to a minimum in the middle of the deeper Rose Dome cores, and they tend to be higher at the top and bottom of the cores. Again this suggests that the highest sum of olivine and phlogopite occur in the middle of

TABLE 2—Mineral compositions of the lamproites.

Mica

	92-5 86’1”	**92-5 86’1”**	**92-5 86’1”**	**92-5 86’1”**	**92-5 86’1”**	**92-5 86’1”**	**92-5 86’1”**	**92-5 86’1”**	**92-11 89’2”**	**92-11 89’2”**
SiO_2	41.457	40.737	41.242	28.381	29.151	29.796	30.14	29.638	40.894	40.64
TiO_2	4.994	4.98	5.051	25.97	27.846	27.214	27.7	27.728	5.494	5.14
Al_2O_3	2.946	4.933	1.559	0.047	0.184	0.049	0.112	0.049	7.786	8.203
FeO	11.996	10.274	13.308	2.558	3.078	2.954	2.853	2.198	7.543	7.246
MgO	22.157	22.142	22.126	3.916	2.62	2.382	2.333	3.243	22.299	22.548
CaO	0	0.015	0.023	1.878	2.055	2.011	1.754	1.885	0	0.001
K_2O	9.877	10.225	9.712	5.542	5.725	5.559	5.648	5.916	10.534	10.585
BaO	0.656	0.695	0.269	19.316	16.569	17.202	17.367	17.583	0.115	0.616
Na_2O	0.073	0.056	0.297	6.311	6.169	7.054	6.974	6.888	0.051	0.068
Cr_2O_3	0.079	0.106	0.023					0	0.168	0.25
MnO	0	0.05	0.074	0.343	0.8665	0.715	0.0781	0.517	0.005	0.033
H_2O	3.964	3.988	3.916	3.364	3.436	3.449	3.481	3.477	4.159	4.162
Total	98.199	98.201	97.599	97.625	97.698	98.384	99.142	99.123	99.047	99.491

Mica

	Eagle 4 426’6”	**Eagle 4 426’6”**	**Eagle 4 426’6”**	**Eagle 4 426’6”**	**Eagle 4 426’6”**	**Eagle 4 413’4”**	**Eagle 4 413’4”**	**Eagle 4 413’4”**	**Eagle 4 413’4”**
SiO_2	40.86	40.12	44.37	41.22	40.41	40.597	41.81	40.32	37.9
TiO_2	1.7	2.03	0.93	1.47	1.73	0.364	0.06	2.97	2.05
Al_2O_3	5.5	5.77	7.22	5.05	5.78	5.38	3.006	1.71	0.6
FeO	10.93	11.24	8.9	12.49(Fe_2O_3)	12.68(Fe_2O_3)	16.99	21.4	14.05	24.12
MgO	24.61	23.84	22.07	24.81	24.33	21.11	18.69	23.39	16.72
CaO	0.06	0.03	0.45	0.01	0	0.054	0.12	0	0.02
K_2O	10.65	10.47	7.74	10.68	10.47	10.01	9.94	9.93	9.42
BaO	0.02	0.06	0.63	0.32	0.36	0.006	0.01	0.56	0.07
Na_2O	0.02	0.05	0.1	0.04	0.02	0.24	0.71	0.1	0.2
Cr_2O_3	0.13	0.17	0	0.1	0.15	0.1	0	0.02	0.07
MnO	0.07	0.04	0.16	0.07	0.03	0.34	0.31	0.1	0.54
H_2O	4	3.96	4.07	4.14	4.12	3.93	3.88	3.86	3.59
Total	98.52	97.79	96.64	100.4	100.07	99.13	99.95	97	95.32

Serpentine

	92-5 86’1”	**92-5 86’1”**	**92-5 86’1”**	**92-5 86’1”**	**92-5 86’1”**	**92-5 86’1”**	**92-5 86’1”**	**92-5 86’1”**	**92-5 86’1”**	**92-11 89’2”**
SiO_2	47.224	40.915	43.044	38.249	48.668	46.712	49.845	39.597	42.087	44.92
TiO_2	0.249	0.084	0.049	0.025	0.012	0.196	0	0	0.01	0.29
$Al2O_3$	2.06	0.196	1.058	0.001	2.004	1.997	0.437	0.002	0	3.77
FeO	8.689	6.062	5.042	6.942	9.01	7.511	11.11	5.906	2.36	5.44
MgO	29.549	38.118	37.3	38.961	27.793	30.819	26.935	39.73	41.787	31.37
CaO	0.288	0.179	0.115	0.042	0.446	0.53	0.44	0.048	0.015	0.51
K2O	0.135	0.016	0.022	0.007	0.078	0.123	0.167	0	0.014	0.3
NiO	0.346	0.34	0.228	0.315	0.112	0.391	0.326	0.231	0.479	
Na_2O	0.094	0.046	0.014	0.009	0.074	0.105	0.053	0.007	0.023	0.01
Cr_2O_3	0.063	0.039	0.065	0.052	0.005	0.091	0.018	0	0	
MnO	0.188	0.057	0.142	0.154	0.15	0.177	0.252	0.061	0.026	0.15
H_2O	12.917	12.406	12.712	12.073	12.909	12.918	12.939	12.307	12.757	12.78
Total	101.801	98.458	99.79	96.83	101.261	101.571	102.53	97.89	99.558	99.53

Serpentine

	92-11 89’2”	**92-11 89’2”**	**Eagle 4 426’6”**	**Eagle 4 426’6”**	**Eagle 4 426’6”**	**Eagle 4 426’6”**	**Eagle 4 426’6”**	**Eagle 4 426’6”**
SiO_2	39.19	45.65	44.18	48.64	40.97	41.76	40.53	45.99
TiO_2	0.69	0.46	0.07	0.02	0.01	0.03	0.16	0.98
Al_2O_3	7	5.82	0.75	0	0	0	3.94	6.52
FeO	10.87	8.4	6.46	7.88	4.8	1.46	6.17	8.07
MgO	26.39	23.99	32.73	30.42	38.49	42.12	33.47	23.3
CaO	0.12	0.2	0.39	0.43	0.18	0.01	0.08	0.52
K2O	3.78	2.98	0.05	0.18	0.07	0.01	0.72	6.3
NiO								
Na_2O	0.03	0.08	0.01	0.18	0.06	0.02	0.01	0.13
Cr_2O_3								
MnO	0.07	0.24	0.21	0.15	0.05	0.01	0.15	0.24
H_2O	12.24	12.63	12.39	12.86	12.31	12.65	12.34	12.97
Total	100.38	100.46	97.25	100.76	96.94	98.05	97.53	105.02

TABLE 20 continued

	Olivine		
	Eagle 4 426’6”	**426’6”**	**426’6”**
SiO_2	41.43	41.42	44.37
MgO	50.94	51.51	32.43
CaO	0.04	0.05	0.33
MnO	0.11	0.15	0.17
FeO	8.45	8.43	6.59
Total	100.97	101.56	83.88

	Rutile		
	92-5 86’1”	**92-5 86’1”**	**92-11 89’2”**
SiO_2	1.295	1.328	2.31
TiO_2	68.077	69.886	65.84
Al_2O_3	0.064	0.031	0.06
FeO	7.058	6.113	7.04
MgO	0.075	0.039	0.48
CaO	0.066	0.084	0.31
MnO	0.086	0	0.07
Nb_2O_3	0.42	0.434	0.31
NiO			
Cr_2O_3			0
ZnO			
Total	77.141	77.915	76.43

	Spinel			
	92-5 86’1”	**92-5 86’1”**	**92-11 89’2”**	**92-11 89’2”**
SiO_2	0.088	0.025		
TiO_2	3.013	2.556	3.585	2.387
Al_2O_3	3.735	3.158	5.16	2.696
FeO	15.095	14.843	15.138	18.749
Fe_2O_3	7.369	6.648	9.478	7.632
MgO	10.87	10.835	11.037	7.497
CaO	0	0		
MnO	0.496	0.53	0.533	1.348
Cr_2O_3	58.272	59.758	54.664	57.272
V_2O_3	0.156	0.139		
NiO				
ZnO				
Total	99.096	98.493	99.596	97.582

	Spinel		
	Eagle 4 426’6”	**Eagle 4 426’6”**	**Eagle 4 426’6”**
SiO_2			
TiO_2	2.61	2.42	2.55
Al_2O_3	3.26	3.2	3.59
FeO	16.87	16.02	15.3
Fe_2O_3	9.36	9.29	9.36
MgO	9.39	10.03	10.53
CaO			
MnO	0.92	0.95	0.8
Cr_2O_3	56.82	57.84	57.11
V_2O_3			
NiO			
ZnO			
Total	99.23	99.75	99.24

	Feldspar	
	Eagle 4 413’ 4”	**Eagle 4 413’ 4”**
SiO_2	64.79	64.67
Al_2O_3	19.91	19.84
CaO	0.02	0.03
FeO	0.19	0.11
BaO	0.06	0.11
Na_2O	0.05	0.08
K_2O	16.07	15.86
Total	101.1	100.71

	Pyroxene				
	92-5 86’1”	**92-5 86’1”**	**92-5 86’1”**	**92-11 89’2”**	**92-11 89’2”**
SiO_2	53.722	53.628	53.455	53.42	52.496
TiO_2	1.301	1.283	1.566	1.44	1.834
Al_2O_3	0.061	0.02	0.048	0.024	0.147
FeO	2.492	2.444	2.212	2.426	2.042
Fe_2O_3				0	0.585
MgO	16.427	16.392	16.551	16.56	16.133
CaO	24.384	24.346	24.731	24.3	24.533
MnO	0.104	0.04	0.029	0.035	0.046
Na_2O	0.545	0.554	0.45	0.419	0.441
K_2O				0	0.032
Cr_2O3	0.496	0.458	0.385	0.33	0.359
Total	99.559	99.185	99.449	98.96	98.649

	Pyroxene	
	92-11 89’2”	**92-11 89’2”**
SiO_2	53.251	53.443
TiO_2	2.099	1.937
Al_2O_3	0.126	0.091
FeO	2.567	2.032
Fe_2O_3	0	0.208
MgO	16.346	16.739
CaO	24.527	24.814
MnO	0.07	0.108
Na_2O	0.361	0.404
K_2O	0.013	0.001
Cr_2O_3	0.345	0.224
Total	99.705	100

	Amphibole						
	92-5 86’1”	**92-5 86’1”**	**92-5 86’1”**	**92-5 86’1”**	**92-11 89’2”**	**92-11 89’2”**	**92-11 89’2”**
SiO_2	40.573	52.745	53.885	55.422	49.637	50.331	49.968
TiO_2	5.051	4.547	4.503	3.224	8.306	7.096	7.248
Al_2O_3	2.36	0.028	0.017	0.036	0.012	0.043	0.023
FeO	12.789	4.661	4.493	3.397	4.943	4.492	4.65
MgO	22.047	20.168	20.395	20.844	19.741	19.749	19.605
CaO	0	6.095	6.007	6.187	5.838	5.919	5.995
MnO	0.044	0.287	0.322	0.182	0.192	0.22	0.204
Na_2O	0.082	3.785	3.911	3.654	3.57	3.607	3.678
K_2O	10.136	5.31	5.254	5.226	5.329	5.475	5.483
Cr_2O_3	0.086	0	0	0.025	0.039	0.039	0
NiO	0.119	0	0	0.018			
H_2O	1.868	2.088	2.12	2.13	2.069	2.062	2.055
Total	95.155	99.713	100.907	100.345	99.677	99.034	98.908

TABLE 2 continued

	Amphibole		
	92-11 89'2"	**92-11 89'2"**	**92-11 89'2"**
SiO_2	51.015	55.8	51.698
TiO_2	6.886	2.901	6.326
Al_2O_3	0.025	0.164	0.031
FeO	4.201	2.624	4.288
MgO	20.031	21.908	19.845
CaO	6.168	6.086	6.193
MnO	0.216	0.068	0.114
Na_2O	3.634	3.909	3.613
K_2O	5.509	5.523	5.316
Cr_2O_3	0	0.037	0
NiO			
H_2O	2.081	2.152	2.083
Total	99.765	101.171	99.505

			Apatite		
	92-5 86'1"	**92-5 86'1"**	**92-5 86'1"**	**92-11 89'2"**	**92-11 89'2"**
P_2O5	36.824	40.677	40.502	41.315	27.69
SiO_2	0.674	0.862	0.876	0.727	14.83
Y_2O_3		0.007	0.006	0.038	0.012
SO_3					
MgO	0.068	0.045	0.058	0.078	5.977
CaO	47.749	52.504	52.78	52.962	36.193
MnO	0	0	0	0	0.087
FeO	0.388	0.076	0.092	0.067	1.483
SrO	5.696	2.491	2.309	2.344	4.97
La_2O_3	0.089	0.499	0.498		
Ce_2O_3	0.276	0.803	0.738	1.001	0.242
Na_2O	1.075	0.013	0	1.772	1.683
H_2O	1.617	1.753	1.756		
Cl	0.026	0.025	0		
Nd_2O_3	0	0.555	0.268		
Total	94.432	100.32	99.898	100.305	93.166

	Cyrkelite	**(Ba(Zr).Ti)Si_3O_9**
	92-11 89'2"	**92-11 89'2"**
SiO_2	38.756	38.67
CaO	0.005	0.77
TiO_2	0.468	1.86
ZrO_2	25.527	23.79
HfO_2	0.385	0.48
BaO	32.865	33.08
Total	98.006	98.65

	Perovskite			
	92-11 89'2"	**92-11 89'2"**	**92-11 89'2"**	**92-11 89'2"**
SiO_2	0.01	0	1.05	0.03
TiO_2	51.94	52.18	51.76	54.71
Al_2O_3				
FeO	1.2	1.01	1.08	0.75
MgO	0.01	0.02	0.22	0.02
CaO	32.91	33.48	35.36	36.39
Na_2O	0.46	0.43	0.57	0.37
Cr_2O_3	1.56	1.55	0.91	0.98
Nb_2O_3	0.39	0.43	0.53	0.37
ZrO_2	0.07	0.1	0.06	0
SrO	1.67	1.74	2.06	1.76
Ta_2O_5	0.05	0.02		0.01
La_2O_3	2.06	1.77	1	1
Ce_2O_3	4.92	4.28	2.09	2.24
Total	97.23	97	96.69	98.64

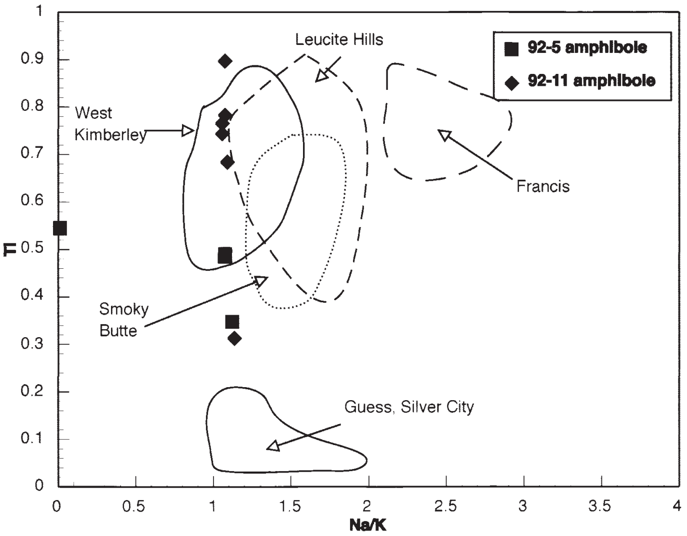

FIGURE 4—The cationic Ti and Na/K ratios of amphiboles from cores 92-5 and 92-11 are compared to other lamproites (Mitchell and Bergman 1991).

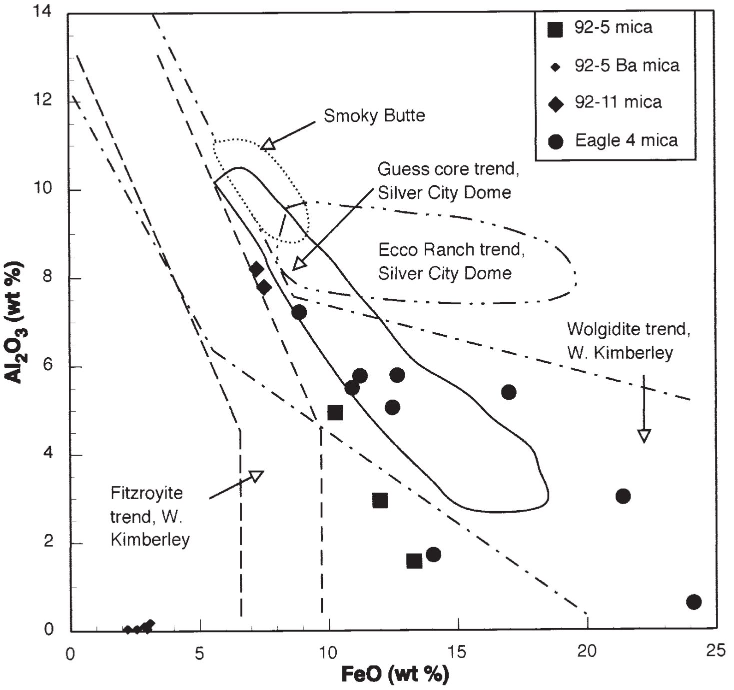

FIGURE 5—The Al_2O_3 and FeO compositions (weight percent) of micas from cores 92-5 and 92-11 (Silver City Dome) and Eagle 4 (Rose Dome) are compared to other lamproites (Mitchell and Bergman, 1991).

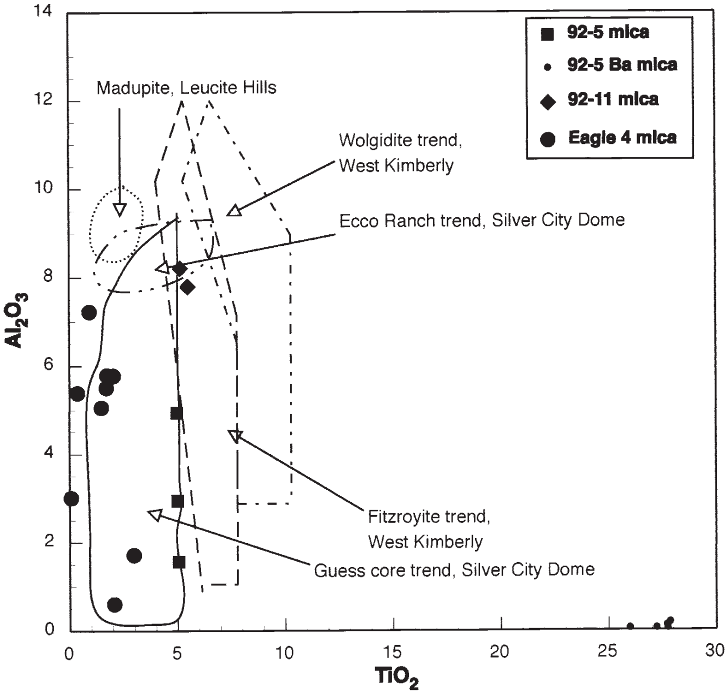

FIGURE 6—The Al_2O_3 and TiO_2 composition (weight percent) of micas from cores 92-5, 92-11, and Eagle 4 are compared to other lamproites (Mitchell and Bergman, 1991).

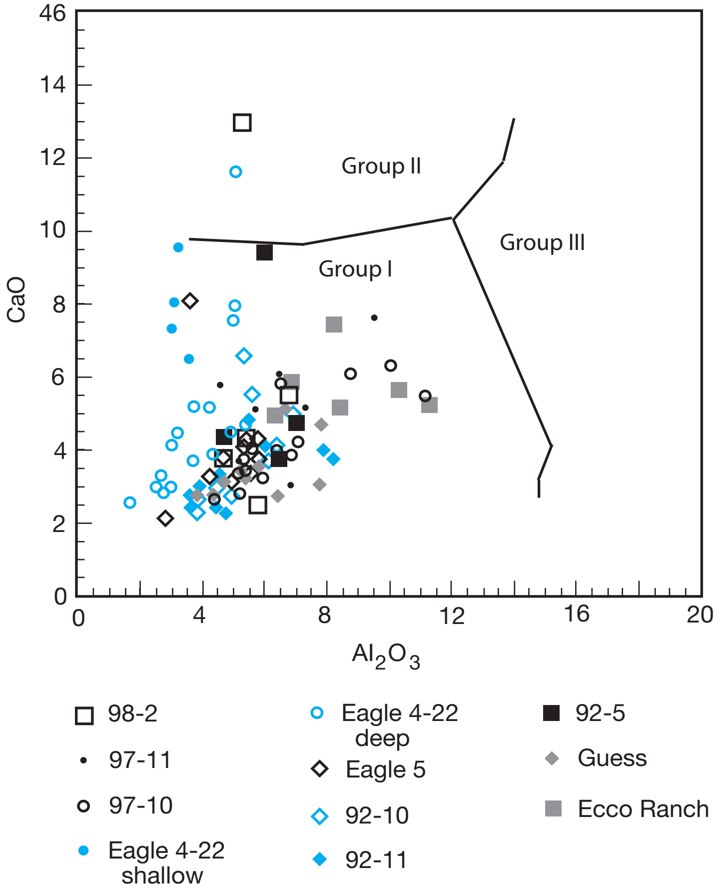

FIGURE 7—The composition of CaO in all samples is plotted against Al_2O_3. Most samples of the Kansas lamproites plot in the Group I field. These lamproites formed in continental settings with mild extension (Foley et al., 1987; Foley, 1994). Samples plotting in Group II are komafugites from continental rift zones. Samples plotting in Group III are ultrapotassic rocks from active orogenic regions.

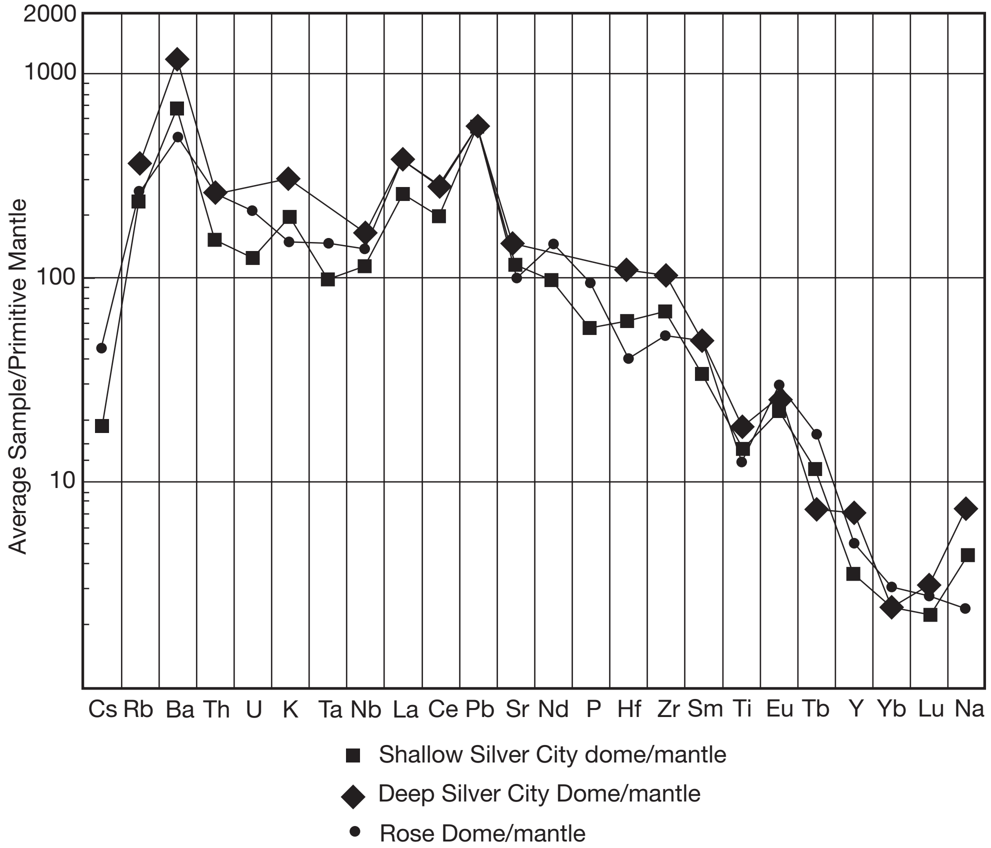

FIGURE 8—Concentration of the average values of the Silver City and Rose Dome lamproites are normalized to primitive mantle (McDonough et al., 1992).

these cores with lesser sums of these minerals occurring at the top and bottom. The highest Na_2O again may be due to a concentration of perovskite, shcherbakovite, or K-richterite. The fairly good correlation of TiO_2 and Na_2O in Eagle 4–22 suggest that perovskite and shcherbakovite may be important controls on these element oxides. The poor correlation of TiO_2 with Na_2O in Eagle 5 suggests that only K-richterite may be the main control. Also P_2O_5 correlates with CaO (fig. 12) as at Rose Dome, again suggesting that apatite is a major control for these elements.

Elemental Trends vs. Mg#

There are systematic trends of some element concentrations vs. Mg# (examples in figs. 15 and 16). The concentration of some elements clearly increase with decreasing Mg# (fig. 15; SiO_2 [in most cores], TiO_2, Al_2O_3, and K_2O with correlation coefficients ranging from 0.7 to 0.75). Note, however, that the SiO_2 content of many samples from the Eagle 4 core decrease with decreasing Mg# (fig. 15). Some elements tend to more poorly increase with decreasing Mg# (fig. 15; CaO, P_2O_5, Sc, Ta, Zr, Hf, Th, and REE with correlation coefficients ranging from 0.28 to 0.65). A few elements tend to decrease with decreasing Mg# (fig. 16; MgO, Ni, LOI, Co, Cr). Other elements have little or no correlation with Mg#.

The inverse correlation of SiO_2, TiO_2, Al_2O_3, and K_2O with Mg# should be due to gradual removal of ferromagnesian minerals (olivine and phlogopite with lesser diopside and richterite,) and possibly removal of perovskite and shcherbakovite. The direct correlation of MgO, Ni, Co, and Cr with Mg# should also be due to the removal of ferromagnesian minerals (especially olivine).

Discussion

Formation of the Primary Magmas

Metasomatized mantle near the lower portion of the Precambrian mantle lithosphere has been hypothesized to melt to form lamproites (Foley, 1992; Foley, 1993; Mitchell, 1995; Sato, 1997; Mitchell and Edgar, 2002). The exact depth of melting is uncertain. Olivine lamproites containing diamonds, however, ought to form at depths in excess of 130 to 150 km (Mitchell and Bergman, 1991; Foley, 1993; Edgar and Mitchell, 1997; Sato, 1997). Also the low Al_2O_3 content and high LREE/HREE ratios of olivine lamproites require garnet to remain in the source as the magma forms (Sato, 1997). The sources are likely to be metasomatized lherzolites to harzbergites that have been enriched in varied amounts of veins containing clinopyroxene, K-Ti amphibole, phlogopite, apatite, and K-Ba-Zr-Nb titanates (Jaques et al., 1986; Bergman, 1987; Mitchell and Bergman, 1991; Foley, 1993). The likely wide variation in the amount of veins versus the lherzolite-harzburgite melting can explain the wide variation in the composition of lamproites (Mitchell, 1995) even in a small area such as those at the Silver City and Rose domes (tables 11 and 12). The lower SiO_2 and Al_2O_3 and higher MgO lamproites at Rose Dome likely result from the higher-temperature melting of a higher proportion of lherzolite-harzburgite and less vein material compared to the more SiO_2-rich and MgO-poor lamproites at the

TABLE 3—The composition of lamproites and associated sedimentary rocks of Woodson County.

	92-5 Core-Silver City Dome										
	Limestones		**Lamproites**								
Depth (feet; inches)	**63’7”**	**65’1”**	**65’3”**	**66’1”**	**70’5”**	**71’7”**	**74’8”**	**78’2”**	**81’6”**	**85’6”**	**86’1”**
Depth (meters)	**19.38**	**19.84**	**19.89**	**20.14**	**21.46**	**21.82**	**22.76**	**23.83**	**24.84**	**26.06**	**26.24**
SiO_2	19.09	5.69	48.56	47.51	48.46	47.76	44.64	45.45	44.66	44.51	46.44
TiO_2	0.05	0.07	3.52	3.4	2.89	2.78	3.49	3.28	2.86	3.21	3.25
Al_2O_3	0.51	1.11	5.92	6.48	7.07	7.08	5.51	4.86	5.33	4.95	5.59
Fe_2O_3(total)	2.58	5.14	7.46	7.96	7.02	6.78	8.40	8.58	7.95	8.21	8.29
MnO	0.18	0.16	0.16	0.12	0.09	0.10	0.14	0.13	0.13	0.12	0.11
MgO	2.21	3.95	15.09	17.09	16.49	16.84	19.2	22.21	22.35	22.58	21.91
CaO	41.92	45.27	3.88	3.76	4.51	4.75	4.7	4.35	3.27	3.57	3.31
Na_2O	2.68	0.12	2.48	1.94	1.78	1.59	1.37	1.80	1.71	1.92	1.82
K_2O	0.34	0.10	6.83	6.84	7.56	6.91	5.42	3.68	4.34	3.8	3.93
P_2O_5	11.97	0.05	0.08	0.06	0.09	0.07	1.15	0.91	0.82	0.81	0.51
LOI	17.75	37.85	4.20	3.60	3.70	4.46	4.45	4.25	5.85	4.55	4.00
Total	99.45	99.64	99.32	99.07	99.90	99.37	99.00	99.93	99.99	99.03	99.82
Rb	13	6.7	137	133	154	151	156	115	150	116	101
Ba	887	268	10322	1952	1539	1348	2240	2450	5229	5804	4759
Sr	861	1030	1050	1160	867	1180	3025	1810	1975	2210	1880
Th	0.59	0.78	13.3	13.5	8.7	9.7	29.5	14.9	12.3	13.8	13.5
Hf	0.26	0.31	22.6	22.3	22.4	21.3	21.1	19.7	18.8	19.5	19.9
Zr	13.9	13.3	912	890	910	906	1106	841	739	801	804
Ta	0.04	0.08	4.6	4.5	3.7	3.4	4.4	4.2	3.7	3.8	4.0
Co	2.9	5.0	42.2	44.4	46.1	42.8	49.2	52.2	59.2	58.1	53.5
Sc	4.1	3.4	15.7	14.9	52.6	13.3	14.5	13.5	11.4	14.0	14
Ni	19	25.8	524	581	640	578	714	754	875	845	743
Cr			889	958	889	958	899	1160	1170	1070	1070
U	2.06	3.91	2.82	2.62	2.38	1.72	3.5	4.19	2.83	2.94	2.8
Y	5.2	5.0	17.5	16.4	13.5	13.4	13.6	19.4	14.1	16.0	15.3
Nb	0.95	1.1	94	95	66	52	90	93	74	83	79
La	3.0	2.9	170	177	146	132	219	221	202	208	198
Ce	6.5	6.0	313	347	318	264	448	452	375	402	388
Pr	0.77	0.8	33.5	39.0	37.8	30.5	49.1	51.2	40.5	43.0	42.5
Nd	3.1	3.2	109	127	128	102	158	171	137	149	142
Sm	0.68	0.77	16.2	15.2	13.8	12.0	15.1	20	14.4	16.0	15.8
Eu	0.57	0.27	8.09	4.05	3.48	3.10	3.17	4.87	2.90	3.18	3.05
Gd	0.71	0.77	9.95	9.23	8.26	7.49	9.54	12.3	9.79	10.3	9.94
Tb	0.11	0.11	1.27	1.21	1.07	1.21	1.17	1.47	1.22	1.25	1.26
Dy	0.59	0.68	4.34	3.95	3.30	3.42	3.35	4.58	3.43	3.86	3.71
Ho	0.13	0.12	0.70	0.64	0.54	0.52	0.56	0.8	0.55	0.66	0.58
Er	0.29	0.34	1.69	1.47	1.26	1.25	1.24	1.68	1.33	1.49	1.48
Tm							0.18		0.18	0.19	0.19
Yb	0.28	0.25	1.30	1.18	0.91	0.83	1.30	1.28	1.10	1.30	1.20
Lu	0.040	0.030	0.20	0.18	0.14	0.13	0.17	0.2	0.16	0.16	0.16
Cu	6.7	10.7	58.5	63.3	52.4	36.6	58.7	56.5	44.8	47.4	50
Li							46		30	32	35
Zn	6.6	20.2	70.4	80	59	62.7	92	87.5	70	71.9	80
Cs	0.20	0.11	0.25	0.28	0.37	0.45	0.29	0.24	0.50	0.30	0.22
Ga	4.5	7.1	15.4	17.4	16.6	15.9	17.5	18.0	14.0	14.4	15.5
Ge							2		1	1	1
Pb	6.1	3.7	41.0	41.7	27.0	8.3	42.2	44.4	40.6	42.4	37.3
V	342	32.3	197	112	77.7	56.8	79	49.2	42.8	45	38.6
K_2O/Na_2O	0.13	0.83	2.75	3.53	4.25	4.35	3.96	2.04	2.54	1.98	2.16
$(K_2O+Na_2O)/Al_2O_3$	9.37	0.28	1.94	1.64	1.57	1.43	1.47	1.43	1.41	1.47	1.30
Mg#	0.485	0.458	0.690	0.703	0.721	0.732	0.715	0.740	0.756	0.752	0.744

TABLE 3 continued

	92-5 Core-Sliver City Dome						
	Lamproites					**Limestone**	**Altered carbonate shale**
Depth (feet; inches)	**91’5”**	**92’4”**	**96’1”**	**99’8”**	**103’6”**	**107’1”**	**109’4”**
Depth (meters)	**27.86**	**28.14**	**29.29**	**30.38**	**31.55**	**32.64**	**33.32**
SiO_2	44.86	44.97	44.4	45.64	46.58	11.18	40.21
TiO_2	3.17	2.96	3.55	3.4	3.34	0.03	0.76
Al_2O_3	5.22	5.11	5.98	5.82	5.68	0.33	13.89
Fe_2O_3(total)	7.67	7.75	7.07	7.72	7.22	4.64	5.07
MnO	0.11	0.11	0.13	0.10	0.14	0.24	0.09
MgO	20.94	22.79	12.84	18.88	18.38	3.99	7.62
CaO	3.58	3.2	9.44	4.21	3.33	42.1	13.29
Na_2O	1.66	1.61	2.44	1.83	1.66	0.77	1.34
K_2O	4.54	4.27	5.11	5.52	5.19	0.06	5.27
P_2O_5	0.71	0.45	2.78	1.31	1.11	0.13	0.1
LOI	5.55	5.00	4.93	4.11	5.5	35.85	12.25
Total	99.05	99.07	99.09	99.02	99.28	99.42	100.03
Rb	112	128	69	97	118	3	189
Ba	8220	6890	1558	3400	9732	112	539
Sr	2170	1560	2600	1400	1760	881	819
Th	12.7	10.2	17.1	11.7	10.3	0.38	7.7
Hf	18.9	17.4	22.3	21.9	20.2	0.16	2.68
Zr	742	687	899	880	803	5.4	112
Ta	3.6	3.2	3.9	4.1	3.6	0.04	1.06
Co	55.6	58.5	39.2	44.6	50.6	2.4	14.7
Sc	14.6	13.3	14.5	14.3	13.3	2.43	12.8
Ni	794	925	344	620	838	15	48.7
Cr	1020	1160	772	1094	895	6	111
U	2.7	2.57	5.2	2.65	2.45	1.68	3.12
Y	14.9	12.5	25.4	23.4	17.8	4.0	14.2
Nb	76	62	82	84	76	0.64	17.6
La	197	147	196	176	167	2.6	28.8
Ce	381	299	423	335	291	5.3	46.3
Pr	42.2	34.4	52.3	36.6	30.9	0.6	5.3
Nd	144	121	203	119	106	2.4	19.8
Sm	15.2	14.1	29.8	17.1	12.4	0.49	3.7
Eu	2.88	2.67	6.80	5.29	2.04	0.16	0.85
Gd	10.1	9.23	18.0	11.3	8.38	0.53	3.0
Tb	1.24	1.05	2.06	1.45	1.17	0.079	0.44
Dy	3.61	3.09	6.12	5.33	4.21	0.49	2.23
Ho	0.60	0.52	1.04	0.89	0.68	0.11	0.39
Er	1.41	1.13	2.17	2.08	1.71	0.29	1.25
Tm	0.18	0.14	0.27		0.19		
Yb	1.20	1.00	1.60	1.40	1.15	0.27	1.25
Lu	0.13	0.13	0.21	0.19	0.15	0.05	0.19
Cu	49.2	44.2	54.9	64.8	25	2.3	15.0
Li	40	37	95		61		
Zn	71.4	74.4	64	76.1	61	5.2	65.9
Cs	0.19	0.25	0.16	0.17	0.27	0.083	9.5
Ga	17.2	14.8	15.7	15.3	15.8	1.33	18.3
Ge	1	1	1		2		
Pb	36.0	31.8	58.2	38.7	35.6	2.0	5.8
V	94	68	129	146	131	18.1	113
K_2O/Na_2O	2.73	2.65	2.09	3.02	3.13	0.08	3.93
$(K_2O+Na_2O)/Al_2O_3$	1.46	1.42	1.60	1.54	1.47	4.04	0.57
Mg#	0.750	0.764	0.666	0.729	0.737	0.486	0.623

TABLE 3 continued

	92-11 Core-Silver City Dome									
	Limestones			**Lamproites**						
Depth (feet; inches) **Depth (meters)**	**58’3”** **17.68**	**60’5”** **18.42**	**61’3”** **18.67**	**62’0”** **18.90**	**65’4”** **19.91**	**69’11”** **21.31**	**74’2”** **22.61**	**78’4”** **23.88**	**79’10”** **24.33**	**84’7”** **25.78**
SiO_2	1.6	1.74	5.88	49.7	45.95	44.84	44.96	42.88	41.88	41.75
TiO_2	0.04	0.03	0.08	4.24	3.38	3.66	3.59	2.42	2.48	2.16
Al_2O_3	0.28	0.38	0.56	8.24	6.04	5.63	7.96	4.00	3.66	3.64
Fe_2O_3(total)	2.26	0.41	0.59	7.9	8.09	8.38	7.79	7.93	8.12	8.03
MnO	0.07	0.03	0.05	0.10	0.13	0.13	0.10	0.14	0.12	0.13
MgO	3.01	1.28	1.04	12.45	18.87	19.61	15.97	26.21	27.95	29.04
CaO	50.93	53.44	51.21	3.83	3.93	3.78	4.04	3.09	2.84	2.50
Na_2O	0.02	0.03	0.58	1.15	1.88	1.76	0.85	1.09	0.85	0.67
K_2O	0.03	0.05	0.14	8.40	5.75	5.37	8.59	3.82	2.97	2.70
P_2O_5	0.03	0.04	0.6	0.03	0.44	0.28	1.14	0.98	0.77	0.66
LOI	40.95	42.7	38.75	3.15	4.13	5.15	3.95	6.15	7.09	7.6
Total	99.34	100.26	99.66	99.41	99.01	99.41	99.32	99.36	99.27	99.39
Rb	0.6	5.6	14.2	137	133	127	246	169	136	133
Ba	45	29	91	1447	2190	6590	2369	4289	3357	3147
Sr	1120	1250	1680	718	2030	1615	1430	2260	2050	2000
Th	0.23	0.21	0.44	8.2	15.1	16.1	12.3	11.2	11.0	9.6
Hf	0.11	0.15	0.22	26.8	21.9	23.4	26.6	14.8	13.8	12.5
Zr	8.2	5.5	5.9	1067	873	896	1073	598	560	548
Ta	0.03	0.03	0.06	5.0	4.3	4.5	6.0	3.3	3.1	2.7
Co	2.5	1.8	2.1	41.2	49.3	54.2	39.5	65.9	67.2	72.6
Sc	2.3	2.7	3.1	16.4	14.3	14.6	19.7	10.4	10.6	10.1
Ni	21.3	15.4	15.6	331	687	680	405	1071	1114	1278
Cr	5.4	4.0	6.7	788	1026	995	821	1140	1020	1150
U	2.85	0.88	1.5	2.38	2.84	3.3	2.37	2.09	2.4	2.0
Y	1.1	1.4	1.9	12.5	17.2	18.5	19.7	13.1	13.3	11.4
Nb	0.4	0.4	0.9	99	93	96	100	69	70	60
La	0.89	0.94	2.03	209	177	229	191	172	157	141
Ce	1.88	1.93	4.23	388	360	451	399	327	304	275
Pr	0.22	0.24	0.52	39.9	41.3	47.8	45.7	35.0	32.7	29.9
Nd	0.94	0.93	1.99	124	137	161	149	118	110	99.5
Sm	0.17	0.20	0.35	11.3	16.0	17.9	16.5	13.1	12.3	11.3
Eu	0.05	0.05	0.09	2.16	4.18	3.44	4.43	2.64	2.44	2.20
Gd	0.18	0.19	0.34	7.43	9.56	11.5	10.5	8.58	8.06	7.08
Tb	0.03	0.03	0.05	0.93	1.25	1.46	1.40	1.01	1.03	0.89
Dy	0.15	0.17	0.26	2.35	4.16	4.50	4.73	2.90	3.26	2.73
Ho	0.03	0.04	0.05	0.44	0.66	0.76	0.82	0.50	0.51	0.44
Er	0.06	0.13	0.14	1.24	1.59	1.84	1.86	1.13	1.21	1.11
Tm				0.19		0.23		0.14	0.16	0.15
Yb	0.07	0.13	0.13	1.29	1.27	1.50	1.55	0.99	1.10	0.90
Lu	0.01	0.02	0.02	0.16	0.18	0.19	0.23	0.11	0.13	0.13
Cu	3.2	0.01	0.01	75.3	60.6	55.9	80.8	41.2	43.1	37.7
Li				22		18		42	46	40
Zn	6.3	1.0	4.1	81	79.7	75.6	87.3	62.2	68.3	77.7
Cs	0.02	0.11	0.22	0.21	0.32	0.29	0.69	1.26	1.1	1.07
Ga	3.0	1.0	0.72	17.7	16.1	17	18.9	9.9	10.6	9.6
Ge				2		1		1	1	1
Pb	2.0	0.57	2.5	29.8	41.9	51.8	7.4	24.3	34.6	27.2
V	20.4	21.9	31.6	168	136	96	25.1	32.3	29.7	30.4
K_2O/Na_2O	1.50	1.67	0.24	7.30	3.06	3.05	10.11	3.50	3.49	4.03
$(K_2O+Na_2O)/Al_2O_3$	0.23	0.27	1.97	1.33	1.54	1.55	1.34	1.48	1.26	1.11
Mg#	0.594	0.774	0.660	0.634	0.720	0.720	0.693	0.784	0.791	0.799

TABLE 3 continued

92-11 Core-Silver City Dome

Lamproites

Depth (feet; inches)	**89’2”**	**91’10”**	**96’2”**	**102’1”**	**105’5”**	**108’9”**	**114’6”**
Depth (meters)	**27.18**	**27.99**	**29.31**	**31.12**	**32.13**	**33.15**	**34.90**
SiO_2	42.66	43.41	43.57	43.25	44.19	44.82	45.06
TiO_2	2.00	2.3	2.56	2.45	2.51	2.86	3.49
Al_2O_3	3.84	4.86	4.63	4.68	4.58	5.19	5.62
Fe_2O_3(total)	7.93	7.72	7.6	7.49	7.58	7.56	8.04
MnO	0.12	0.11	0.10	0.13	0.12	0.12	0.12
MgO	28.43	26.07	25.9	26.14	25.88	22.74	19.19
CaO	2.76	2.29	3.30	2.93	2.48	2.97	4.75
Na_2O	0.87	1.21	1.32	1.21	1.39	1.18	2.01
K_2O	3.09	4.98	4.00	3.47	3.69	4.95	4.70
P_2O_5	0.79	0.50	0.81	0.61	0.30	0.64	0.97
LOI	7.00	5.30	5.25	6.25	6.22	5.62	5.12
Total	99.94	99.37	99.63	99.25	99.57	99.55	99.42
Rb	132	193	126	151	143	163	100
Ba	2130	4752	2396	4412	4465	6810	1732
Sr	2330	1430	3460	2020	1800	2140	1730
Th	7.0	9.8	8.7	9.9	9.7	11.6	14.4
Hf	12.7	14.9	17	14.1	14.2	17.8	24.1
Zr	569	582	707	577	577	702	1000
Ta	2.6	2.8	3.0	2.9	2.6	3.1	4.3
Co	64.8	66	60.2	63.2	64.6	56.6	52.4
Sc	10.6	10.4	12.3	10.7	10.5	12.5	15.6
Ni	1222	1040	1070	1145	1133	903	736
Cr	1640	961	1230	977	1050	916	1026
U	1.19	1.41	1.48	2.25	2.17	2.54	2.94
Y	9.6	12.1	10.6	11.5	11.2	13.5	17.4
Nb	51	56	55	59	59	67	90
La	123	144	150	156	156	177	187
Ce	244	285	290	291	307	340	381
Pr	27.2	32.4	32.3	31.9	33.6	37.0	43.8
Nd	89	111	106	106	115	127	144
Sm	10.4	12.4	11.9	11.9	12.5	14.3	16.3
Eu	2.98	2.24	3.52	2.33	2.37	2.78	3.95
Gd	5.81	7.82	7.02	7.64	7.89	9.29	9.72
Tb	0.78	0.98	0.89	0.93	0.93	1.14	1.29
Dy	2.18	3.05	2.59	2.71	2.59	3.37	4.14
Ho	0.33	0.49	0.40	0.44	0.42	0.54	0.66
Er	0.83	1.09	0.93	1.02	0.94	1.31	1.59
Tm		0.13		0.13	0.14	0.17	
Yb	0.66	0.90	0.76	0.90	0.90	1.10	1.25
Lu	0.09	0.11	0.12	0.12	0.11	0.16	0.17
Cu	48.3	28	48.5	40.0	38.2	45.4	61.7
Li		35		34	29	28	
Zn	66.4	62.6	63.9	58.3	76.9	64.9	77.9
Cs	0.76	0.98	0.86	0.86	0.72	0.57	0.25
Ga	10.8	13.0	12.7	11.4	12.9	14.3	17.8
Ge		1		1	1	1	
Pb	18.0	20.1	14.7	28.7	28.7	34.7	50.1
V	30.2	46.3	30.8	41.4	46.1	64.6	128
K_2O/Na_2O	3.55	4.12	3.03	2.87	2.65	4.19	2.34
$(K_2O+Na_2O)/Al_2O_3$	1.24	1.52	1.40	1.23	1.37	1.41	1.49
Mg#	0.798	0.788	0.789	0.793	0.790	0.768	0.724

TABLE 3 continued

	92-10 Core-Silver City Dome									
	Limestones		**Lamproites**							
Depth (feet; inches)	**28’3”**	**29’8”**	**30’6”**	**32’10”**	**37’5”**	**40’6”**	**45’3”**	**48’6”**	**51’4”**	**55’0”**
Depth (meters)	**8.61**	**9.04**	**9.30**	**10.01**	**11.40**	**12.34**	**13.79**	**14.78**	**15.65**	**16.76**
SiO_2	1.83	1.95	45.65	48.22	42.49	44.64	44.62	43.22	44.39	43.03
TiO_2	0.03	0.06	3.94	3.74	3.58	4.36	3.14	3.03	3.00	2.34
Al_2O_3	0.39	0.53	5.37	6.12	7.3	6.98	6.39	5.68	5.37	3.91
Fe_2O_3(total)	0.41	0.44	8.40	8.48	8.39	9.07	7.91	7.95	7.90	8.16
MnO	0.04	0.03	0.10	0.08	0.08	0.09	0.11	0.10	0.12	0.19
MgO	0.49	0.72	14.59	16.25	17.83	15.86	19.74	22.00	21.55	26.91
CaO	54.32	53.67	6.59	4.12	4.87	4.89	4.15	3.93	3.72	2.95
Na_2O	0.02	0.03	0.70	0.66	0.72	0.75	0.87	0.93	0.82	0.58
K_2O	0.06	0.06	4.55	5.49	6.42	5.90	5.29	4.81	5.07	3.37
P_2O_5	0.05	0.08	2.03	2.07	2.06	2.24	2.29	1.99	1.72	1.28
LOI	42.25	42.2	6.80	4.46	4.95	4.34	4.13	4.95	4.89	6.45
Total	100.04	100.00	99.14	100.12	99.03	99.53	99.09	99.12	99.19	99.65
Rb	4	3.0	102	132	156	130	123	124	147	133
Ba	311	1041	2434	2610	1790	2310	2535	3050	4270	2890
Sr	1200	1290	1740	1690	1570	1830	2010	2250	2150	1900
Th	0.35	0.39	16.0	14.8	15.3	20.2	16.9	11.7	12.3	11.1
Hf	0.13	0.21	18.8	20.4	20.4	24.1	18.9	18.2	18.4	14.3
Zr	4.4	9.0	74	781	826	1096	803	737	704	580
Ta	0.03	0.06	5.6	4.6	3.8	5.5	4.4	4.0	3.8	3.2
Co	1.7	2.1	38.7	43.8	49.1	50.1	53.2	47.9	54.1	72.0
Sc	2.5	2.6	14.4	13.6	15.2	19.2	13.7	14.8	13.3	10.8
Ni	14.9	13.7	433	515	539	409	691	714	770	1243
Cr			684	1230	1090	930	1290	1300	1180	833
U	1.19	1.2	2.34	2.25	3.3	4.9	3.4	3.25	2.8	2.3
Y	3.2	2.4	15.0	15.9	17.1	22.4	20.6	16.4	14.6	13.4
Nb	0.45	0.9	117	88	89	127	90	70	86	70
La	2.0	2.1	220	227	200	261	227	164	180	160
Ce	3.7	3.3	427	452	379	476	438	324	341	306
Pr	0.51	0.41	47.8	51.6	41.1	51.9	47.5	36.4	37.7	33.1
Nd	1.9	1.5	153	169	138	175	163	120	129	112
Sm	0.37	0.31	17.0	18.8	14.1	20.0	18.2	13.6	14.5	12.2
Eu	0.20	0.42	4.52	4.33	3.04	4.34	3.96	4.05	2.99	2.60
Gd	0.39	0.30	10.3	11.3	9.62	13.1	12.0	8.32	9.67	8.01
Tb	0.065	0.050	1.33	1.44	1.24	1.60	1.46	1.10	1.20	1.00
Dy	0.36	0.29	3.93	4.13	3.65	5.19	4.85	3.53	3.63	3.06
Ho	0.076	0.059	0.61	0.64	0.63	0.84	0.81	0.62	0.59	0.50
Er	0.22	0.18	1.37	1.42	1.59	1.99	1.91	1.56	1.34	1.22
Tm					0.21	0.26	0.23		0.16	0.15
Yb	0.18	0.18	1.07	1.08	1.50	1.8	1.40	1.33	1.00	1.00
Lu	0.03	0.03	0.15	0.16	0.17	0.23	0.21	0.19	0.11	0.11
Cu	0.13	5.1	82.7	69.6	54.0	83.0	53.0	44.5	49.3	40.2
Li					30	21	24		41	71
Zn	9.1	13	85.8	83.8	71.3	95	70	71	71.3	70
Cs	0.02	0.02	0.21	0.25	0.25	0.38	0.39	0.35	0.46	0.65
Ga	0.44	2.2	16.1	18.6	16.3	18.7	15.0	16.5	13.7	10.4
Ge					1	1	1		1	1
Pb	1.6	2.6	24.6	37.0	46.9	60.3	46.4	26.4	36.6	32.0
V	14	13.4	131	64	140	177	146	235	72	58
K_2O/Na_2O	3.00	2.00	6.50	8.32	8.92	7.87	6.08	5.17	6.18	5.81
$(K_2O+Na_2O)/Al_2O_3$	0.25	0.22	1.13	1.15	1.11	1.09	1.12	1.19	1.27	1.18
Mg#	0.568	0.643	0.656	0.678	0.700	0.658	0.733	0.753	0.750	0.784

TABLE 3 continued

	92-10 Core-Silver City Dome							
	Lamproites						**Limestones**	
Depth (feet; inches)	**57’2”**	**60’3”**	**64’7”**	**67’2”**	**70’8”**	**71’11”**	**72’4”**	**74’6”**
Depth (meters)	**17.42**	**18.36**	**19.69**	**20.47**	**21.54**	**21.92**	**22.05**	**22.71**
SiO_2	42.21	42.43	42.51	42.94	43.23	41.75	1.37	1.5
TiO_2	2.32	2.34	2.25	2.30	2.66	3.20	0.02	0.02
Al_2O_3	4.43	3.91	3.86	3.87	5.02	5.65	0.23	0.08
Fe_2O_3(total)	7.84	7.96	7.99	7.86	7.76	6.43	0.36	0.64
MnO	0.14	0.15	0.15	0.14	0.12	0.08	0.03	0.04
MgO	27.43	27.9	28.09	27.64	26.11	24.43	1.04	1.2
CaO	2.94	2.62	2.44	2.38	2.76	5.56	53.61	53.19
Na_2O	0.61	0.51	0.55	0.64	0.9	1.33	0.03	0.03
K_2O	3.63	3.39	3.23	3.57	3.85	2.16	0.03	0.03
P_2O_5	1.17	0.99	0.97	0.85	0.92	2.31	0.05	0.03
LOI	6.30	6.95	6.90	6.50	5.70	5.85	42.7	42.65
Total	99.53	99.69	99.42	99.18	99.39	99.12	99.59	99.53
Rb	132	118	119	108	118	44	3.1	3.1
Ba	3190	3520	2810	3074	1525	756	31	51
Sr	1940	1850	1990	1840	2110	2950	1210	1170
Th	9.9	9.9	9.2	9.1	10.6	9.2	0.26	0.11
Hf	13.6	13.9	14.1	13.8	16.7	19.6	0.08	0.08
Zr	554	567	590	559	670	830	1.9	5.2
Ta	2.9	2.9	2.6	2.7	3.1	3.5	0.03	0.02
Co	66.2	75.2	72.3	72.7	53.0	24.2	1.9	2.6
Sc	10.2	10.5	9.8	10.0	11.3	14.0	2.4	2.2
Ni	1086	1350	1313	1317	890	171	16.9	24.5
Cr	1190	1180	994	898	1300	547	5.3	4.1
U	2.0	2.1	2.0	1.9	2.14	2.14	1.45	1.01
Y	11.2	12.4	11.7	11.8	14.2	16.0	1.5	0.9
Nb	59	62	59	56	70	78	0.32	0.29
La	147	154	151	141	149	229	1.2	0.84
Ce	284	296	294	271	303	519	2.2	1.6
Pr	31.1	32.7	31.3	29.6	34.7	62.6	0.3	0.2
Nd	104	110	106	98.1	114	198	1.1	0.71
Sm	11.4	12.0	11.5	10.8	13.0	20.0	0.22	0.11
Eu	2.36	2.46	2.31	2.21	3.35	4.43	0.05	0.05
Gd	7.43	7.68	7.48	7.21	7.86	12.1	0.21	0.10
Tb	0.91	0.94	0.94	0.90	1.03	1.57	0.03	0.01
Dy	2.75	2.82	2.84	2.80	3.20	4.15	0.19	0.09
Ho	0.42	0.48	0.46	0.44	0.53	0.64	0.04	0.02
Er	1.03	1.15	1.13	1.09	1.23	1.41	0.12	0.05
Tm	0.13	0.15	0.14	0.15				
Yb	0.90	0.90	1.00	0.89	0.98	1.08	0.09	0.05
Lu	0.09	0.13	0.13	0.13	0.14	0.15	0.01	0.01
Cu	44.8	38.1	39.4	40.7	45.5	59.4	1.1	4.4
Li	57	71	66	66				
Zn	58	66	62.4	61.6	67.8	55.5	9.8	11.5
Cs	0.49	0.47	0.43	0.39	0.55	0.14	0.04	0.07
Ga	12.1	11.5	10.3	11.5	12.6	15.6	0.67	3.4
Ge	1	1	1	1				
Pb	26.0	23.8	29.3	25.2	31.4	5.3	0.89	0.55
V	43	42.7	41.4	71.7	46.5	139	11.3	12.3
K_2O/Na_2O	5.95	6.65	5.87	5.58	4.28	1.62	1.00	1.00
$(K_2O+Na_2O)/Al_2O_3$	1.11	1.15	1.14	1.27	1.13	0.80	0.36	1.02
Mg#	0.794	0.794	0.795	0.795	0.787	0.807	0.761	0.673

TABLE 3 continued

97-10 Core-Silver City Dome

Lamproites

Depth (feet; inches)	**38’0”**	**41’10”**	**50’9”**	**53’8”**	**58’7”**	**61’1”**	**65’2”**	**70’2”**	**72’7”**	**79’11”**	**83’9”**
Depth (meters)	**11.58**	**12.75**	**15.47**	**16.36**	**17.86**	**18.62**	**19.86**	**21.39**	**22.12**	**24.36**	**25.53**
SiO_2	45.22	46.53	46.25	47.29	46.1	48.95	43.83	44.59	44.90	43.87	44.04
TiO_2	3.70	3.84	3.85	3.70	3.59	2.97	3.53	2.84	2.56	2.85	2.73
Al_2O_3	6.62	6.89	10.10	7.09	8.89	11.21	5.09	5.33	4.43	5.11	4.97
Fe_2O_3(total)	7.90	7.74	6.58	8.08	6.95	6.31	8.21	7.76	7.82	7.81	7.87
MnO	0.11	0.12	0.09	0.11	0.12	0.07	0.15	0.12	0.15	0.11	0.11
MgO	14.32	14.95	7.12	14.92	7.86	6.86	20.81	22.77	23.55	24.16	24.69
CaO	5.82	3.81	6.26	4.18	6.05	5.48	3.73	3.10	2.63	3.37	2.89
Na_2O	1.65	1.28	0.94	1.55	0.85	0.84	1.52	1.43	1.28	1.61	1.53
K_2O	7.54	8.45	10.90	8.08	9.19	10.55	6.26	5.49	5.05	4.24	4.40
P_2O_5	2.04	0.96	3.27	0.19	1.78	2.93	0.45	0.41	0.52	0.50	0.39
LOI	3.60	3.20	2.85	2.81	3.81	1.74	4.29	4.63	5.95	5.06	5.05
Total	99.06	99.01	99.35	99.14	99.07	99.19	99.04	99.29	99.57	99.58	99.38
Rb	121	136	154	162	<2	132	210	198	240	132	156
Ba	2650	9200	6530	9300	4810	8440	8800	5200	5510	4470	4330
Sr	2040	1820	3500	895	28302	2860	1620	2000	1790	3270	1900
Th			14.7	12	25.6	6.3	13.8	10.1	11.6	10	
Hf			19	22	19	15	19	17	18	16	
Zr			782	866	772	561	746	625	618	576	
Ta			8	4.4	4.6	3	3.9	3.2	4.8	3.3	
Co			26.8	46.9	42	45.6	85.5	58.5	75.5	59.3	
Sc			15	16	15	16	14	12	11	12	
Ni			64	515	129	73	749	884	1185	932	
Cr			95	739	258	177	1260	1240	1440	1240	
U			2.22	3.41	2.6	1.68	3.43	2.26	2.9	2.34	
Y	22	19	18.2	23	28	16.9	21	16	13.8	14.5	17
Nb			116	96	93	67	106	73	62	74	
La			444	202	297	178	186	158	154	140	
Ce			1080	392	688	346	359	310	275	269	
Pr			95.1	45.4	60.9	40.9	39.6	34.6	30.3	29.7	
Nd			301	159	197	142	132	112	114	97.6	
Sm			28.6	19	20.9	15.7	15.6	13.4	11.6	10.6	
Eu			6.98	6.17	5.4	5.06	5.38	3.90		3.24	
Gd			20.6	14.9	15	11.8	12.2	10.1	8.67	7.85	
Tb			2.24	1.7	1.67	1.27	1.41	1.13	1.14	0.96	
Dy			4.5	5.08	4.1	3.49	4.06	3.29	3.25	3.06	
Ho			0.66	0.85	0.69	0.60	0.64	0.55	0.57	0.52	
Er			1.47	2.04	1.66	1.58	1.66	1.33	1.55	1.3	
Tm			0.17	0.25	0.22	0.20	0.20	0.15	0.18	0.16	
Yb			1.3	1.6	1.66	1.3	1.5	1.1	1.2	1.1	
Lu			0.18	0.22	0.19	0.18	0.19	0.16	0.23	0.15	
Cu			57	52	42	36	51	38	44	32	
Li			11	31	12	12	35	38	37	34	
Zn			71	79	60	45	64	58	71	65	
Cs			0.2	0.3	0.2	0.3	0.5	0.6	0.8	0.6	
Ga			20	17	18	16	15	13	10	11	
Ge			2	2	2	1	2	1	1	1	
Pb			36	56	68	11	53	34	48	44	
V			65	103	111	52	35	43	59	32	
K2O/Na_2O	4.57	6.60	11.60	5.21	10.81	12.56	4.12	3.84	3.95	2.63	2.88
$(K_2O+Na_2O)/Al_2O_3$	1.64	1.63	1.32	1.59	1.28	1.14	1.82	1.56	1.71	1.42	1.46
Mg#	0.666	0.680	0.543	0.670	0.554	0.545	0.736	0.763	0.768	0.773	0.775

TABLE 3 continued

97-10 Core-Silver City Dome

Lamproites

Depth (feet; inches)	**89’7”**	**93’3”**	**98’7”**	**102’10”**	**108’10”**	**110’10”**
Depth (meters)	**27.31**	**28.42**	**30.05**	**31.34**	**33.17**	**33.78**
SiO_2	44.00	44.33	43.56	46.10	43.88	47.35
TiO_2	2.79	2.79	3.02	3.11	3.33	3.4
Al_2O_3	5.25	5.28	5.32	6.00	5.43	5.38
Fe_2O_3(total)	7.98	7.93	7.92	7.70	7.82	7.89
MnO	0.12	0.12	0.12	0.10	0.12	0.12
MgO	24.01	23.85	22.61	19.22	20.02	19.14
CaO	2.84	3.02	3.25	3.22	4.39	4.48
Na_2O	1.61	1.63	1.61	1.70	1.66	1.48
K_2O	4.65	4.68	5.41	5.84	5.68	5.47
P_2O_5	0.34	0.36	0.52	0.28	1.37	1.01
LOI	4.87	4.92	4.83	5.15	4.22	4.02
Total	99.16	99.65	99.17	99.40	99.33	100.44
Rb	168	168	173	122	104	103
Ba	4300	4650	6480	7150	7300	2950
Sr	1820	1880	2300	2660	5000	3110
Th			11.6	13.5		
Hf			18	21		
Zr			687	731		
Ta			4.3	5.8		
Co			62.6	60.6		
Sc			12	14		
Ni			941	846		
Cr			1220	1310		
U			2.72	2.14		
Y	18	15	16.5	13.8	19	15
Nb			84	54		
La			190	224		
Ce			356	402		
Pr			39.1	42.9		
Nd			130	138		
Sm			14.6	15.4		
Eu			4.49			
Gd			10.8	11.0		
Tb			1.27	1.30		
Dy			3.43	3.19		
Ho			0.56	0.54		
Er			1.36	1.49		
Tm			0.18	0.18		
Yb			1.1	1.1		
Lu			0.17	0.14		
Cu			41	43		
Li			30	21		
Zn			69	68		
Cs			0.6	0.3		
Ga			14	14		
Ge			2	4		
Pb			46	43		
V			36	62		
K_2O/Na_2O	2.89	2.87	3.36	3.44	3.42	3.70
$(K_2O+Na_2O)/Al_2O_3$	1.46	1.47	1.60	1.52	1.64	1.55
Mg#	0.768	0.768	0.758	0.733	0.738	0.727

TABLE 3 continued

	97-11 Core-Silver City Dome									
	Mudstone	**Lamproites**								
Depth (feet; inches)	**74’4”**	**75’3”**	**80’1”**	**87’8”**	**88’8”**	**98’5”**	**98’8”**	**100’10”**	**106’4”**	**112’**
Depth (meters)	**22.7**	**22.9**	**24.4**	**26.7**	**27.0**	**30.0**	**30.1**	**30.7**	**32.4**	**34.1**
SiO_2	49.94	46.1	44.96	45.7	43.22	43.08	45.0	43.4	42.8	43.75
TiO_2	0.77	3.58	4.15	3.13	3.88	3.37	2.22	2.60	3.01	2.88
Al_2O_3	20.34	7.07	5.87	9.67	4.67	5.12	7.42	4.67	4.65	5.05
Fe_2O_3(total)	3.86	7.92	8.68	6.75	8.99	8.12	6.49	7.84	7.81	7.78
MnO	0.03	0.11	0.12	0.05	0.13	0.17	0.09	0.12	0.12	0.12
MgO	2.74	15.72	17.78	9.35	20.54	21.35	16.64	22.02	23.05	23.81
CaO	2.72	4.58	4.48	7.58	5.77	4.24	5.14	3.69	3.72	3.25
Na_2O	0.41	1.67	1.57	0.49	1.64	1.60	0.55	1.41	1.51	1.66
K_2O	11.67	7.23	7.08	10.83	4.91	5.87	9.82	5.35	5.25	4.86
P_2O_5	0.45	1.43	0.75	0.03	1.46	0.88	1.03	1.16	0.75	0.49
LOI	3.5	3.45	3.28	5.3	3.57	4.26	3.40	6.45	5.32	4.75
Total	98.53	99.24	99.08	99.33	99.31	99.13	98.37	99.54	98.79	99.22
Rb	201	100	140	160	140	230	253	225	205	184
Ba	15481	1390	1510	3060	1720	7550	3560	5120	5370	5470
Sr	3120	1880	1660	906	2860	1920	1450	2190	1680	1800
Th		13.1		17.1	15.9	14.3		12.1		10.5
Hf		22		58	22	19		19		16
Zr		878		2310	893	731		640		589
Ta		3.9		8.5	4.9	4.6		3.6		3.7
Co		63.5		39.3	53.1	88.2		68.5		62.9
Sc		15		20	15	14		12		12
Ni		514		98	703	762		971		948
Cr		1020		257	1040	1380		1185		1300
U		1.85		2.61	3.12	3.28		2.62		2.35
Y	36	18.9	20	2	22	21	18	12.9	17	14.6
Nb		77		155	104	106		57		80
La		219		26.9	260	247		186		147
Ce		424		54.9	487	472		347		278
Pr		46.8		6.16	55.2	52.4		39.1		30.9
Nd		155		20.9	183	174		133		102
Sm		17.7		2.2	19.8	19.3		14.8		11.6
Eu		4.07		1.04	4.57	5.78				3.81
Gd		13.2		1.61	14.9	14.7		10.2		8.9
Tb		1.52		0.20	1.67	1.61		1.25		1.09
Dy		4.36		0.68	4.56	4.38		3.06		3.14
Ho		0.73		0.17	0.74	0.73		0.50		0.52
Er		1.64		0.66	1.81	1.74		1.37		1.28
Tm		0.21		0.12	0.24	0.24		0.16		0.16
Yb		1.3		1.1	1.5	1.5		0.90		1.1
Lu		0.19		0.13	0.19	0.21		0.18		0.15
Cu		48		5	72	42		55		37
Li		135		13	132	62		56		59
Zn		60		44	87	86		67		53
Cs		0.3		0.4	0.2	0.5		0.6		0.5
Ga		17		12	20	15		14		12
Ge		2		2	2	2		2		1
Pb		69		5	57	51		22		39
V		123		16	43	18		17		25
K_2O/Na_2O	28.46	4.33	4.51	22.10	2.99	3.67	17.85	3.79	3.48	2.93
$(K_2O+Na_2O)/Al_2O_3$	0.65	1.50	1.75	1.30	1.72	1.76	1.55	1.74	1.76	1.58
Mg#	0.438	0.686	0.693	0.604	0.715	0.743	0.738	0.755	0.765	0.771

TABLE 3 continued

97-11 Core-Silver City Dome (continued)

Lamproites

Depth (feet;inches) **Depth(meters)**	**121’7”** **37.1**	**127’3”** **38.8**	**131’10”** **40.2**	**136’2”** **41.5**	**141’2”** **43.0**	**145’4”** **44.3**	**146’5”** **44.6**	**148’5”** **45.2**
SiO_2	44.38	45.46	44.8	44.13	45.69	44.1	44.63	43.94
TiO_2	2.76	3.15	3.28	3.41	2.84	3.01	3.62	3.35
Al_2O_3	5.30	6.04	5.75	5.02	6.90	5.85	6.64	6.58
Fe_2O_3(total)	7.88	7.69	7.70	7.81	7.07	7.21	8.01	7.80
MnO	0.12	0.12	0.12	0.12	0.11	0.11	0.10	0.14
MgO	22.81	20.53	20.47	20.43	16.95	17.31	18.02	16.37
CaO	3.18	3.30	3.44	4.14	3.06	5.17	4.08	6.04
Na_2O	1.59	1.56	1.71	2.02	1.28	1.61	1.60	1.42
K_2O	5.46	6.02	5.99	5.17	7.80	7.04	7.14	7.56
P_2O_5	0.46	0.33	0.38	0.80	1.41	2.45	1.39	1.12
LOI	4.49	3.63	4.02	4.64	4.72	5.55	3.32	4.79
Total	99.21	98.93	98.89	99.05	99.19	100.03	99.07	99.32
Rb	196	153	134	129	133	150	135	130
Ba	5060	7670	7870	9970	9720	2010	1870	915
Sr	1820	2060	3010	2060	2350	3360	2620	899
Th	9.6	11.6	12.8			20.7	15.5	10.6
Hf	17	18	19			1	21	21
Zr	652	711	720			150	871	788
Ta	3.1	4.8	4.3			8.2	4.4	5.5
Co	75.3	217	54.6			56.9	71.1	47.8
Sc	12	13	13			13	15	15
Ni	934	787	765			784	620	565
Cr	1070	1020	1160			1160	1010	969
U	2.35	2.43	2.78			2.76	3.01	2.98
Y	16	16	18.4	18	15	15.7	18.9	13
Nb	70	82	91			65	95	98
La	184	201	204			256	247	162
Ce	357	384	394			495	461	313
Pr	39.3	42.9	43.5			52.2	49.6	33.4
Nd	130	140	142			175	160	109
Sm	14.3	15.2	15.6			18.2	16.8	12.1
Eu	4.11	4.81	5.13			4.24	4.02	2.81
Gd	10.9	11.4	12.2			12.6	13.7	9.25
Tb	1.16	1.26	1.34			1.49	1.54	1.06
Dy	3.24	3.46	3.72			3.64	3.86	2.67
Ho	0.49	0.58	0.60			0.60	0.62	0.45
Er	1.22	1.39	1.51			1.57	1.53	1.23
Tm	0.15	0.16	0.18			0.18	0.20	0.19
Yb	1.1	1.2	1.3			1.0	1.4	1.3
Lu	0.14	0.15	0.17			0.29	0.19	0.20
Cu	41	44	43			74	70	55
Li	51	42	42			54	85	68
Zn	56	61	59			67	70	64
Cs	0.5	0.3	0.3			0.4	0.3	0.4
Ga	12	13	13			15	17	15
Ge	1	1	2			1	2	2
Pb	38	41	47			49	52	70
V	21	29	34			193	183	1140
K_2O/Na_2O	3.43	3.86	3.50	2.56	6.09	4.37	4.46	5.32
$(K_2O+Na_2O)/Al_2O_3$	1.61	1.50	1.62	1.78	1.53	1.76	1.56	1.60
Mg#	0.761	0.746	0.745	0.742	0.725	0.725	0.712	0.698

TABLE 3 continued

	97-11 Core-Silver City Dome (continued)			**98-2 Core-Silver City Dome**							
	Apatite?	**Limestones**		**Lamproites**							
Depth (feet; inches)	**148’11”**	**153’3”**	**155’6”**	**33’8”**	**43’7”**	**46’1”**	**51’2”**	**60’9”**	**64’4”**	**69’4”**	**79’2”**
Depth (meters)				**10.26**	**13.28**	**14.05**	**15.06**	**18.52**	**19.61**	**21.13**	**24.13**
SiO_2	4.12	6.71	12.63	44.95	43.99	45.23	44.42	37.03	44.71	44.3	42.74
TiO_2	0.05	0.06	0.07	3.87	3.30	3.49	3.58	4.34	3.54	3.01	2.84
Al_2O_3	0.31	0.2	2.3	6.86	5.91	5.85	5.75	5.39	5.60	4.77	5.19
Fe_2O_3(total)	1.82	4.13	5.67	7.78	7.65	7.92	7.80	8.44	8.26	7.95	7.72
MnO	0.1	0.2	0.21	0.11	0.12	0.12	0.12	0.13	0.12	0.12	0.12
MgO	1.52	3.58	4.8	13.86	17.98	19.53	18.74	13.52	20.59	22.33	23.07
CaO	47.61	45.03	39.05	5.47	3.83	2.48	3.26	12.95	3.94	3.75	3.51
Na_2O	0.95	0.37	0.52	0.85	0.68	0.65	0.97	0.50	0.54	0.51	0.74
K_2O	0.46	0.22	1.9	8.51	7.33	6.53	6.67	6.17	5.64	4.68	4.87
P_2O_5	35.4	0.07	0.02	1.38	2.03	0.91	1.16	2.42	0.39	0.7	0.61
LOI	3.5	37.75	32.7	4.65	4.95	5.39	5.41	7.69	4.57	6.48	5.16
Total	96.27	98.49	99.99	99.01	99.02	99.64	99.23	99.23	99.00	99.53	97.45
Rb	<2	<2	96	127	165	150	139	130	152	196	194
Ba	1340	258	287	4240	8420	11540	9570	1720	7780	6945	5230
Sr	2340	1210	758	2080	2620	2150	2360	3880	1970	2400	2500
Th				31		14.1			13.8	15.4	10.9
Hf				25		20			19	22	15
Zr				964		814			767		593
Ta				4.9		4.3			4.7	0.8	3.1
Co				42.1		52.1			54.8	53.7	76.1
Sc				16		14			14	12	11
Ni				418		684			748	939	895
Cr				897		1010	958	684	835	1130	1300
U				2.49		3.3			3.61	1.2	2.7
Y	13	<2	<2	13	19	19.5	19	25	19.5	19	15.1
Nb				100		94			107		75
La				187		198			188	176	145
Ce				369		380			366	353	277
Pr				40.1		42.4			41.2	39.8	30.3
Nd				128		140			137	134	100
Sm				13.5		15.4			16.7	14.9	10.9
Eu				3.89		5.7			5.47	4.2	3.56
Gd				10.5		12.4			12.6	10.5	8.78
Tb				1.12		1.39			1.45	1.33	1.04
Dy				2.57		3.64			4.04	3.74	2.88
Ho				0.41		0.63			0.66	0.66	0.5
Er				1.07		1.52			1.6	1.73	1.23
Tm				0.17		0.19			0.21		0.15
Yb				1.2		1.3			1.4	1.3	1.2
Lu				0.16		0.19			0.19	0.16	0.15
Cu				55		41			48		37
Li				62		45			32		18
Zn				69		68			72		54
Cs				0.2		0.4			0.3		0.8
Ga				17		15			15		12
Ge				1		1			2		1
Pb				51		34			53		43
V				98		82			31		28
K_2O/Na_2O				10.01	10.78	10.05	6.88	12.34	10.44	9.18	6.58
$(K_2O+Na_2O)/Al_2O_3$				1.55	1.53	1.39	1.53	1.39	1.25	1.24	1.25
Mg#				0.662	0.721	0.731	0.725	0.638	0.733	0.755	0.767

TABLE 3 continued

	98-2 Core-Silver City Dome (continued)		**Eagle 4-22-Rose Dome**					
	Lamproites		**Lamproites**				**Limestone**	
Depth (feet; inches)	**89'4"**	**100'7"**	**43'10"**	**45'8"**	**47'4"**	**47'9"**	**396'4"**	**408'8"**
Depth (meters)	**27.23**	**30.66**	**13.36**	**13.92**	**14.43**	**14.55**	**120.77**	**124.56**
SiO_2	45.5	43.94	37.85	38.2	36.97	38.14	19.77	2.17
TiO_2	2.63	3.23	2.35	2.81	2.62	2.61	0.11	0.02
Al_2O_3	4.92	6.05	3.39	3.69	3.25	3.24	2.19	0.01
Fe_2O_3(total)	7.58	7.65	7.76	9.32	10.05	10.15	0.81	0.39
MnO	0.12	0.12	0.20	0.09	0.12	0.105	0.02	0.02
MgO	22.32	18.69	20.58	23.8	22.31	22.28	1.08	0.72
CaO	2.79	3.79	9.51	6.49	8.01	7.30	41.46	52.86
Na_2O	0.83	1.43	0.35	0.37	0.33	0.33	0.08	0.04
K_2O	5.24	6.21	3.48	2.42	2.56	2.53	0.5	0.02
P_2O_5	0.32	1.44	2.10	2.09	1.84	1.86	0.13	0.22
LOI	7.33	4.57	11.11	9.35	10.5	9.95	32.95	42.15
Total	100.25	97.99	99.21	99.11	99.20	99.19	99.24	98.83
Rb	207	130	112.5	81	93	94	<2	<2
Ba	4990	5430	2715	2200	3560	4030	66	20
Sr	1700	2260	1975	1950	2030	2035	1110	1730
Th	12.1	13.1	21.3			21.8		
Hf	18	18	4			11		
Zr	620	726	423			732	<2	14
Ta	0.9	3.7	8.2			6.2		
Co	56.8	82.6	48.4			68.9		
Sc	12	13	15.0			16		
Ni	1040	703	884			1320		
Cr	1195	955	1180	1230	1160	1130		
U	2.42	3.03	3.17			4.27		
Y	16	13	19.6	24	24	22.3	<2	<2
Nb	37	89	72			82	<2	<2
La	155	155	219			245		
Ce	311	305	437			487		
Pr	34.6	33.4	48.7			53.7		
Nd	114	109	164			186		
Sm	12.5	11.6	18.9			21.6		
Eu	3.5	3.84	4.48			5.41		
Gd	8.86	9.04	13.2			15.6		
Tb	1.09	1.05	1.62			1.87		
Dy	2.87	2.62	4.38			5.11		
Ho	0.5	0.40	0.71			0.83		
Er	1.37	1.08	1.89			2.03		
Tm	0.16	0.16	0.20			0.23		
Yb	1	1.1	1.2			1.4		
Lu	0.17	0.16	0.18			0.18		
Cu	39	48	83			82		
Li	17	25	33			24		
Zn	61	56	56			75		
Cs	0.6	0.3	0.5			0.7		
Ga	12	13	10			10		
Ge	2	2	2			2		
Pb	38	55	38			44		
V	41	146	40			8		
K_2O/Na_2O	6.31	4.34	9.94	6.54	7.76	7.67		
$(K_2O+Na_2O)/Al_2O_3$	1.43	1.50	1.28	0.87	1.02	1.01		
Mg#	0.764	0.729	0.745	0.737	0.709	0.707		

TABLE 3 continued

Eagle 4-22-Rose Dome (continued)								
	Lamproites							
Depth (feet; inches)	**411’11”**	**416’11”**	**418’11”**	**419’6”**	**422”**	**423’5”**	**426’5”**	**429’10”**
Depth (meters)	**125.55**	**127.08**	**127.69**	**127.86**	**128.63**	**129.06**	**129.97**	**131.01**
SiO_2	36.73	42.58	41.45	37.54	41.13	41.76	40.1	38.46
TiO_2	7.06	2.42	3.37	4.14	2.73	2.29	2.06	1.62
Al_2O_3	5.15	4.32	5.09	5.14	4.98	4.38	3.75	2.61
Fe_2O_3(total)	11.69	8.97	8.68	9.83	8.73	8.33	8.03	8.04
MnO	0.14	0.16	0.18	0.135	0.16	0.15	0.13	0.14
MgO	12.71	22.91	20.39	20.90	23.45	25.71	26.95	30.55
CaO	11.63	5.19	7.62	7.95	4.54	3.89	3.78	3.05
Na_2O	1.38	1.39	1.42	1.40	1.16	0.74	0.5	0.19
K_2O	5.63	3.58	4.18	4.17	4.20	4.33	4.1	3.59
P_2O_5	3.63	1.23	1.40	3.03	1.84	1.58	1.35	1.35
LOI	3.25	5.86	4.34	4.47	5.92	6.7	7.85	8.60
Total	99.90	99.13	99.24	99.76	99.17	100.26	99.04	99.16
Rb	172.5	149	148	137	198	223	211	177
Ba	5080	2585	8080	6660	1040	1300	1560	6975
Sr	2845	1960	1825	2630	2340	2180	2250	1730
Th	42	23.1	29.7		31.1			16
Hf	1	18	22		12			12
Zr	817	644	1050		605			449
Ta	31.6	1.9	7.6		2.2			0.5
Co	40.7	61.7	48.8		63			73.1
Sc	37	15	27		14			12
Ni	128	1110	477		1030			1470
Cr	781.5	1205	1005	1030	1585	1370	1500	1020
U	11.7	5.4	6.53		4.86			3.58
Y	38.1	25.7	29.6	37	22.1	23	22	16.8
Nb	291	85	121		88			41
La	469	240	333		335			176
Ce	872	481	625		710			350
Pr	96.6	52.6	68.1		77.3			39.7
Nd	335	175	235		258			135
Sm	41.6	20.1	27.8		27			15.1
Eu		4.96			6.03			
Gd	29.5	14.8	20.2		18.3			10.2
Tb	3.63	1.92	2.45		2.19			1.28
Dy	10.4	5.52	7.05		5.06			3.51
Ho	1.65	0.92	1.15		0.80			0.54
Er	4.21	2.44	2.99		1.99			1.52
Tm	0.45	0.31	0.34		0.22			0.16
Yb	2.7	1.8	2.0		1.3			1.0
Lu	0.42	0.25	0.32		0.17			0.15
Cu	179	79	168		80			60
Li	22	10	28		15			8
Zn	121	73	53		69			69
Cs	1.1	1.0	0.7		1.1			1.5
Ga	17	16	9		15			7
Ge	2	1	2		1			2
Pb	46	32	26		45			49
V	21	21	7		19			26
K_2O/Na_2O	4.08	2.58	2.94	2.98	3.62	5.85	8.20	18.89
$(K_2O+Na_2O)/Al_2O_3$	1.62	1.43	1.35	1.33	1.30	1.35	1.40	1.61
Mg#	0.545	0.737	0.721	0.700	0.747	0.772	0.787	0.807

TABLE 3 continued

	Eagle 4-22-Rose Dome (continued)								
	Lamproites								
Depth (feet; inches)	**431'8"**	**433'11"**	**438'4"**	**441'9"**	**442'10"**	**443'6"**	**446'**	**448'9"**	**450'10"**
Depth (meters)	**131.57**	**132.26**	**133.60**	**134.65**	**134.98**	**135.18**	**135.94**	**136.78**	**137.41**
SiO_2	38	38.53	38.46	37.47	39.59	38.34	39.15	39.4	41.08
TiO_2	1.88	2.02	2.09	2.12	1.35	3.61	2.81	2.02	1.90
Al_2O_3	3.06	2.75	3.06	3.11	1.73	3.78	3.24	2.64	2.81
Fe_2O_3(total)	7.99	8.23	8.28	8.35	8.57	8.88	9.06	8.36	8.32
MnO	0.13	0.14	0.14	0.16	0.14	0.15	0.14	0.14	0.14
MgO	29.48	29.43	29.48	27.57	31.25	25.01	25.11	29.05	27.78
CaO	3.11	3.41	3.05	4.22	2.64	5.19	4.47	3.1	2.93
Na_2O	0.23	0.28	0.23	0.24	0.31	0.79	0.64	0.36	0.50
K_2O	4.03	4.03	4.07	4.32	2.91	4.38	4.35	4.05	4.80
P_2O_5	1.48	1.59	1.22	1.35	0.96	1.77	1.83	1.11	0.07
LOI	8.85	7.85	8.89	9.54	9.90	6.92	7.88	8.8	8.70
Total	99.00	99.25	99.65	99.06	99.71	99.32	99.07	99.35	99.24
Rb	186	180	196	205	136	167	202	176	199
Ba	5150	6910	5150	3580	1575	1680	1720	1320	1190
Sr	1550	1870	1630	1850	1590	2640	2185	1430	859
Th				20.9	9.6		23.8		15.7
Hf				17	11		10		12
Zr				573	434		767		477
Ta				0.5	0.5		0.5		0.5
Co				64.7	77.8		62.7		69
Sc				13	11		17		12
Ni				1210	1710		1130		1320
Cr	1300	1160	1370	1440	538	1440	1035	750	993
U				3.51	2.98		5.57		3.36
Y	20	21	21	17.8	15.6	30	25.5	21	17.8
Nb				56	37		90		51
La				224	118		274		190
Ce				464	216		558		352
Pr				53.0	24.3		61.4		39.1
Nd				179	83		210		131
Sm				19.9	9.9		24.5		14.7
Eu				4.79	2.42		5.86		3.42
Gd				13.3	7.31		16.7		10.5
Tb				1.64	0.92		2.08		1.32
Dy				4.32	2.74		5.68		3.64
Ho				0.68	0.46		0.91		0.58
Er				1.69	1.24		2.42		1.51
Tm				0.19	0.13		0.25		0.17
Yb				1.2	0.9		1.5		1.0
Lu				0.17	0.11		0.22		0.13
Cu				64	52		86		61
Li				9	13		9		49
Zn				62	91		74		68
Cs				1.1	1.1		1.2		0.9
Ga				9	6		10		8
Ge				2	2		2		2
Pb				37	36		53		33
V				42	75		32		26
K_2O/Na_2O	17.52	14.39	17.70	18.00	9.39	5.54	6.80	11.25	9.59
$(K_2O+Na_2O)/Al_2O_3$	1.55	1.75	1.56	1.63	2.12	1.60	1.78	1.88	2.14
Mg#	0.802	0.797	0.797	0.784	0.800	0.756	0.753	0.793	0.786

TABLE 3 continued

	Eagle 4-22-Rose Dome (continued)				**Eagle 5-Rose Dome**				
	Limestone		**Mudstone**		**Lamproites**				
Depth (feet; inches)	**452’2”**	**452’5”**	**456’5”**	**460’9”**	**364’6”**	**383’4”**	**390’2”**	**398’1”**	**406’3”**
Depth (meters)	**137.82**	**137.90**	**139.11**	**140.43**	**110.10**	**116.84**	**118.92**	**121.34**	**123.83**
SiO_2	2.94	1.1	55.46	55.88	37.0	41.3	39.83	37.82	37.95
TiO_2	0.02	0.03	0.76	0.74	4.08	3.36	2.47	2.26	2.14
Al_2O_3	0.03	0.07	15.54	15.15	3.7	5.49	5.26	4.3	3.6
Fe_2O_3(total)	0.17	0.26	4.93	5.46	11.16	8.38	8.18	8.32	8.56
MnO	0.04	0.01	0.05	0.04	0.19	0.15	0.14	0.14	0.14
MgO	1.2	0.58	2.89	2.63	17.6	21.83	25.63	28.28	29.3
CaO	45.95	54.32	3.97	4.6	8.09	4.28	3.45	3.23	3.84
Na_2O	0.16	0.01	0.46	0.39	0.47	1.08	0.79	0.51	0.37
K_2O	0.01	0.01	10.17	7.11	8.12	6.48	5.88	4.81	3.79
P_2O_5	6.99	0.13	0.22	0.12	4.49	1.89	1.27	1.63	1.7
LOI	34.3	42.85	5.5	7.95	3.38	4.39	5.79	7.25	8.25
Total	92.60	99.57	100.12	100.15	99.13	99.28	99.22	99.03	100.03
Rb	<2	<2	174	169	202	208	206	177	150
Ba	2850	126	1290	494	3810	2920	2830	2120	1130
Sr	4000	1590	248	243	3610	2760	2510	2090	2240
Th					14.4	39.2	25.3	22.7	19
Hf					8	18	12	14	13
Zr		12	135	133	558	663	499	496	503
Ta					8.7	10.2	7.8	7.2	5.9
Co					65.7	59.1	73.6	78.3	80.1
Sc					18	17	12	13	13
Ni					501	641	974.5	1120	1215
Cr					1140	979	1190	1500	1330
U					4.96	4.63	3.86	2.75	3.52
Y	60	<2	50	37	35.7	27.5	16.5	11.0	17.8
Nb		<2	9	11	183.5	134	91.5	86.5	86.5
La					251	462	331	296	241
Ce					446	847	752	606	483
Pr					47.9	99.6	73.6	67.9	54.7
Nd					163	342	248	228	187
Sm					21.1	37.9	25.4	22.1	20.2
Eu					5.97	8.61	5.70	4.87	4.65
Gd					16.3	23.9	15.9	13.5	13.3
Tb					2.04	2.77	1.83	1.51	1.56
Dy					7.19	7.38	4.33	3.07	4.44
Ho					1.225	1.125	0.655	0.475	0.68
Er					3.14	2.48	1.41	1.11	1.51
Tm					0.42	0.29	0.20	0.14	0.20
Yb					2.4	1.9	1.3	1.1	1.2
Lu					0.345	0.245	0.17	0.15	0.155
Cu					80	76	49	54	51
Li					16	23	37	18	11
Zn					90	73	64	50	60
Cs					1.0	1.0	1.5	1.3	1.3
Ga					14	17	13	11	10
Ge					2	2	1	2	1
Pb					25	49	37	40	36
V					42	23	43	90	27
K_2O/Na_2O	0.06				17.28	6.00	7.44	9.43	10.24
$(K_2O+Na_2O)/Al_2O_3$	9.13				2.58	1.60	1.46	1.41	1.31
Mg#	0.886				0.634	0.741	0.775	0.789	0.790

TABLE 3 continued

	Lamproites		**Limestone**	
Depth (feet; inches)	**421’6”**	**427’7”**	**428’3”**	**429’6”**
Depth (meters)	**128.47**	**130.33**	**130.53**	**130.91**
SiO_2	41.6	40.83	11.22	3.3
TiO_2	1.85	2.09	0.18	0.01
Al_2O_3	2.95	2.96	0.95	0.09
Fe_2O_3(total)	8.68	8.09	0.34	0.1
MnO	0.15	0.13	0.03	0.02
MgO	28.71	26.41	4.65	0.54
CaO	2.12	3.39	44.53	53.66
Na_2O	1	1.13	1.65	0.04
K_2O	3.62	4.18	0.16	0.06
P_2O_5	0.62	1.87	30.51	0.1
LOI	8.00	7.00	4.44	41.25
Total	99.91	99.06	99.35	99.42
Rb	120	149	<2	<2
Ba	4900	6520	2060	83
Sr	1150	2170	3920	2030
Th	12.3	14.3	2.1	0.1
Hf	12	13	<1	<1
Zr	438	522	13.7	6.9
Ta	4.4	4.9	<0.5	<0.5
Co	85.5	79.4	1	0.8
Sc	13	14	<5	<5
Ni	1375	1160	15	16.5
Cr	636	960	14	<10
U	3.32	3.37	6.35	1.06
Y	10.6	13.9	10.4	1.9
Nb	83	81.5	5.5	2
La	160	199	84	1.4
Ce	321	384	156	1.9
Pr	35.5	42.6	16.7	0.3
Nd	123	145	55.4	1
Sm	13.6	16	6.3	0.2
Eu	3.85	4.58	1.79	0.11
Gd	8.555	10.6	4.69	0.23
Tb	1.02	1.23	0.59	0.04
Dy	2.64	3.36	2.06	0.21
Ho	0.41	0.535	0.34	<0.05
Er	0.95	1.33	0.72	0.12
Tm	0.12	0.16	0.08	<0.05
Yb	1.1	1.2	0.4	<0.1
Lu	0.145	0.15	0.06	<0.05
Cu	49	59	25	<5
Li	<10	10	<10	<10
Zn	44	54	18	6
Cs	0.7	1.0	<0.1	<0.1
Ga	8	9	2	<1
Ge	2	2	<1	<1
Pb	34	33	12	<5
V	132	277	141	14
K_2O/Na_2O	3.62	3.70	0.10	
$(K_2O+Na_2O)/Al_2O_3$	1.89	2.16	3.04	
Mg#	0.784	0.782	0.938	

TABLE 4—The means and standard deviations of lamproite samples in southeastern Kansas.

	SILVER CITY DOME							
	92-5		**92-11**		**92-10**		**97-10**	
	(14 samples)		**(14 samples)**		**(14 samples)**		**(17 samples)**	
Depth (meters)	**19.9 to 31.5**		**17.75 to 34.9**		**8.61 to 24.9**		**11.6 to 33.8**	
	Mean	**StDev**	**Mean**	**StDev**	**Mean**	**StDev**	**Mean**	**StDev**
SiO_2	45.93	1.52	44.21	2.02	43.67	1.72	45.34	1.57
TiO_2	3.20	0.26	2.86	0.68	3.01	0.69	3.21	0.43
Al_2O_3	5.73	0.72	5.18	1.44	5.28	1.17	6.38	1.94
Fe_2O_3(total)	7.73	0.55	7.87	0.26	8.01	0.58	7.66	0.53
MnO	0.12	0.02	0.12	0.01	0.12	0.03	0.12	0.02
MgO	19.02	3.20	23.18	5.12	22.60	4.99	18.29	6.22
CaO	4.29	1.58	3.25	0.72	3.85	1.28	4.03	1.20
Na_2O	1.83	0.30	1.25	0.40	0.76	0.21	1.42	0.29
K_2O	5.25	1.31	4.75	1.84	4.34	1.21	6.58	2.14
P_2O_5	0.75	0.74	0.64	0.31	1.64	0.57	1.02	0.95
LOI	4.89	1.55	5.57	1.27	5.66	1.02	4.18	1.07
Total	99.30	0.44	99.42	0.21	99.37	0.31	99.34	0.34
Rb	125	25	149	36	120	26	155	38
Ba	4675	3126	3578	1709	2626	871	6004	2108
Sr	1761	639	1930	609	1987	332	3927	6352
Th	13.7	5.1	11.0	2.7	12.6	3.5	12.9	5.1
Hf	20.7	1.6	18.2	5.3	17.5	3.2	18.4	2.1
Zr	855	102	738	201	669	228	696	100
Ta	3.9	0.4	3.6	1.1	3.8	1.0	4.5	1.5
Co	49.4	6.7	58.4	10.0	55.2	14.9	56.3	16.9
Sc	16.7	10.4	12.8	2.9	12.9	2.7	13.7	1.8
Ni	687	155	915	300	817	389	632	410
Cr	1008	125	1053	207	1046	239	898	530
U	3.0	0.9	2.2	0.6	2.6	0.8	2.6	0.6
Y	16.8	3.9	13.7	3.2	15.2	3.3	18.0	3.8
Nb	79.5	12.7	73.1	18.3	80.1	21.4	82.5	20.0
La	183	28	169	28	186	40	217	91
Ce	358	62	332	58	365	82	448	252
Pr	40.2	7.2	36.5	6.3	40.7	10.0	45.9	19.4
Nd	136	28	121	20	135	31	152	59
Sm	16.2	4.4	13.4	2.3	14.8	3.3	16.5	5.2
Eu	4.32	1.80	2.98	0.79	3.35	0.89	5.08	1.20
Gd	10.24	2.56	8.42	1.53	9.43	2.02	12.29	3.73
Tb	1.29	0.25	1.07	0.21	1.19	0.25	1.41	0.37
Dy	4.03	0.85	3.23	0.83	3.61	0.77	3.75	0.66
Ho	0.67	0.15	0.53	0.14	0.59	0.13	0.62	0.10
Er	1.53	0.31	1.26	0.33	1.39	0.29	1.54	0.22
Tm	0.19	0.04	0.16	0.03	0.18	0.05	0.19	0.03
Yb	1.20	0.20	1.08	0.27	1.14	0.27	1.30	0.22
Lu	0.17	0.03	0.14	0.04	0.15	0.04	0.18	0.03
Cu	51.7	8.2	50.3	14.9	53.2	15.3	43.6	7.7
Li	45.0	22.7	32.7	9.3	49.7	20.7	26.1	11.0
Zn	74	9	72	9	71	11	65	9
Cs	0.28	0.10	0.71	0.34	0.39	0.14	0.44	0.21
Ga	16.0	1.2	13.8	3.2	14.2	2.9	14.8	3.1
Ge	1.1	0.4	1.1	0.3	1.0	0.0	1.8	0.9
Pb	37	11	29	13	32	13	44	15
V	90	46	65	47	101	61	60	28
K_2O/Na_2O	2.92	0.81	4.09	2.10	6.06	1.78	5.20	3.24
$(K_2O+Na_2O)/Al_2O_3$	1.51	0.15	1.38	0.13	1.13	0.11	1.52	0.17
Mg#	0.73	0.03	0.76	0.05	0.75	0.05	0.70	0.08

TABLE 4 continued

SILVER CITY DOME								
	97-11 (14 samples)		**98-2 (10 samples)**		**Surface at Silver City-2 (6 samples)**		**Guess-1 (12 samples)**	
Depth (meters)	**22.7 to 45.2**		**10.3 to 30.7**				**305.4 to 312.05**	
	Mean	**StDev**	**Mean**	**StDev**	**Mean**	**StDev**	**Mean**	**StDev**
SiO_2	44.42	0.99	43.68	2.46	44.03	3.22	44.33	3.23
TiO_2	3.19	0.48	3.38	0.50	2.40	0.43	4.41	1.66
Al_2O_3	6.02	1.29	5.63	0.61	4.18	0.25	6.46	0.96
Fe_2O_3(total)	7.74	0.61	7.88	0.28	7.67	0.45	8.53	0.80
MnO	0.12	0.02	0.12	0.00	0.09	0.01	0.13	0.01
MgO	19.01	3.57	19.06	3.32	20.95	2.93	13.00	3.39
CaO	4.40	1.22	4.58	3.05	2.98	0.84	4.67	1.10
Na_2O	1.46	0.39	0.77	0.28	0.50	0.26	2.20	0.57
K_2O	6.67	1.69	6.19	1.17	7.19	1.41	8.99	0.92
P_2O_5	0.96	0.58	1.14	0.69				
LOI	4.41	0.91	5.62	1.15	9.62	1.53	5.46	1.59
Total	99.16	0.35	99.04	0.80	100.27	0.66	99.59	0.70
Rb	165	43	159	30	202	25	279	44
Ba	4696	3009	6587	2853	6595	2133	11229	6206
Sr	2031	669	2392	588			3558	1012
Th	13.7	3.2	15.8	6.9	13.5	2.0	28.2	15.6
Hf	21.1	12.9	19.6	3.2	15.6	2.7	44.7	53.0
Zr	828	507	747	136			1103	39
Ta	5.0	1.7	3.2	1.7	4.4	0.8		
Co	74.9	46.6	59.7	14.3	61.9	6.4	46.1	8.3
Sc	14.1	2.2	13.1	1.7	12.3	1.4	25.2	20.4
Ni	704	240	775	205				
Cr	1048	278	996	189	1585	551	751	302
U	2.7	0.4	2.7	0.8				
Y	16.3	4.5	17.8	3.6			34.0	8.5
Nb	90.0	25.6	83.7	25.3			131.5	13.4
La	195	65	172	20	164.7	26.1	341	155
Ce	372	122	337	39	305.8	56.2	616.4	277.4
Pr	41.0	13.3	37.4	4.6				
Nd	135	44	123	15				
Sm	14.8	4.7	13.6	2.1	13.8	3.0	24.5	13.8
Eu	4.04	1.25	4.31	0.90	2.97	0.39	5.22	3.13
Gd	11.13	3.58	10.38	1.62				
Tb	1.27	0.39	1.21	0.17			0.88	0.45
Dy	3.40	1.03	3.19	0.60				
Ho	0.56	0.16	0.54	0.11				
Er	1.41	0.30	1.37	0.26				
Tm	0.18	0.04	0.17	0.02				
Yb	1.23	0.19	1.21	0.13	0.76	0.04	1.28	0.46
Lu	0.18	0.04	0.17	0.02	0.15	0.02	0.26	0.07
Cu	48.8	18.9	44.7	6.8				
Li	66.6	35.6	33.2	17.5				
Zn	65	12	63	7				
Cs	0.39	0.12	0.43	0.23				
Ga	14.6	2.5	14.0	2.0				
Ge	1.7	0.5	1.5	0.5				
Pb	45	18	46	9				
V	154	317	71	47				
K_2O/Na_2O	5.84	5.44	8.69	2.51	15.75	3.62	4.39	1.41
$(K_2O+Na_2O)/Al_2O_3$	1.62	0.13	1.41	0.12	1.75	0.61	1.91	0.41
Mg#	0.72	0.04	0.72	0.04	0.75	0.03	0.62	0.07

TABLE 4 continued

	SILVER CITY DOME		**ROSE DOME**			
	Ecco Ranch-1		**Eagle 4-22**		**Eagle 5**	
	(9 samples)		**(21 samples)**		**(8 samples)**	
Depth	**237.5 to 247.25**		**13.36 to 137.4**		**110.1 to 130.9**	
	Mean	**StDev**	**Mean**	**StDev**	**Mean**	**StDev**
SiO_2	49.33	2.31	39.09	1.67	39.25	1.85
TiO_2	3.09	0.30	2.66	1.21	2.55	0.77
Al_2O_3	7.78	1.95	3.58	0.95	3.98	0.96
Fe_2O_3(total)	7.15	1.17	8.84	0.94	8.73	1.00
MnO	0.10	0.01	0.14	0.02	0.15	0.02
MgO	13.42	4.69	25.08	4.45	25.86	4.17
CaO	5.00	1.24	5.29	2.51	4.02	1.76
Na_2O	1.83	0.44	0.63	0.45	0.71	0.33
K_2O	8.48	1.56	3.89	0.78	5.13	1.58
P_2O_5			1.65	0.72	1.90	1.13
LOI	3.40	0.88	7.87	2.13	6.47	1.78
Total	100.25	1.20	99.33	0.33	99.35	0.39
Rb	174	28	164	42	173	32
Ba	4484	5325	3527	2247	3165	1867
Sr	2251	498	1969	449	2329	696
Th	11.3	5.0	23.2	8.7	20.8	8.7
Hf	17.7	4.5	11.8	5.9	13.0	2.8
Zr			634	195	519	67
Ta			5.5	9.2	6.9	2.0
Co	46.6	15.6	61.7	11.4	74.9	8.6
Sc	14.3	1.8	17.2	7.9	14.1	2.2
Ni			1072	447	1018	300
Cr	968	299	1153	262	1126	266
U			5.0	2.5	3.7	0.7
Y			23.5	6.0	18.8	8.6
Nb			92.2	70.4	104.1	36.4
La	182.8	44.5	257	95	273	93
Ce	333.0	88.8	505	182	542	181
Pr			55.9	19.8	59.7	20.4
Nd			190	69	203	69
Sm	14.6	4.7	21.9	8.5	22.2	7.3
Eu	2.92	0.92	4.67	1.23	5.37	1.47
Gd			15.42	5.98	14.50	4.57
Tb	0.64	0.19	1.90	0.72	1.70	0.54
Dy			5.22	2.09	4.60	1.78
Ho			0.84	0.33	0.72	0.30
Er			2.18	0.84	1.68	0.74
Tm			0.24	0.09	0.21	0.10
Yb	1.15	0.15	1.45	0.53	1.43	0.47
Lu	0.19	0.03	0.21	0.09	0.19	0.07
Cu			90.4	42.7	58.1	12.5
Li			20.0	12.9	18.1	9.5
Zn			74	19	61	15
Cs			0.99	0.28	1.09	0.24
Ga			10.6	3.7	11.3	2.9
Ge			1.8	0.4	1.8	0.5
Pb			40	8	36	7
V			29	19	83	87
K_2O/Na_2O	5.08	2.32	9.11	5.32	8.78	12.47
$(K_2O+Na_2O)/Al_2O_3$	1.78	0.43	1.50	0.33	1.72	9.48
Mg#	0.66	0.07	0.75	0.06	0.76	14.59

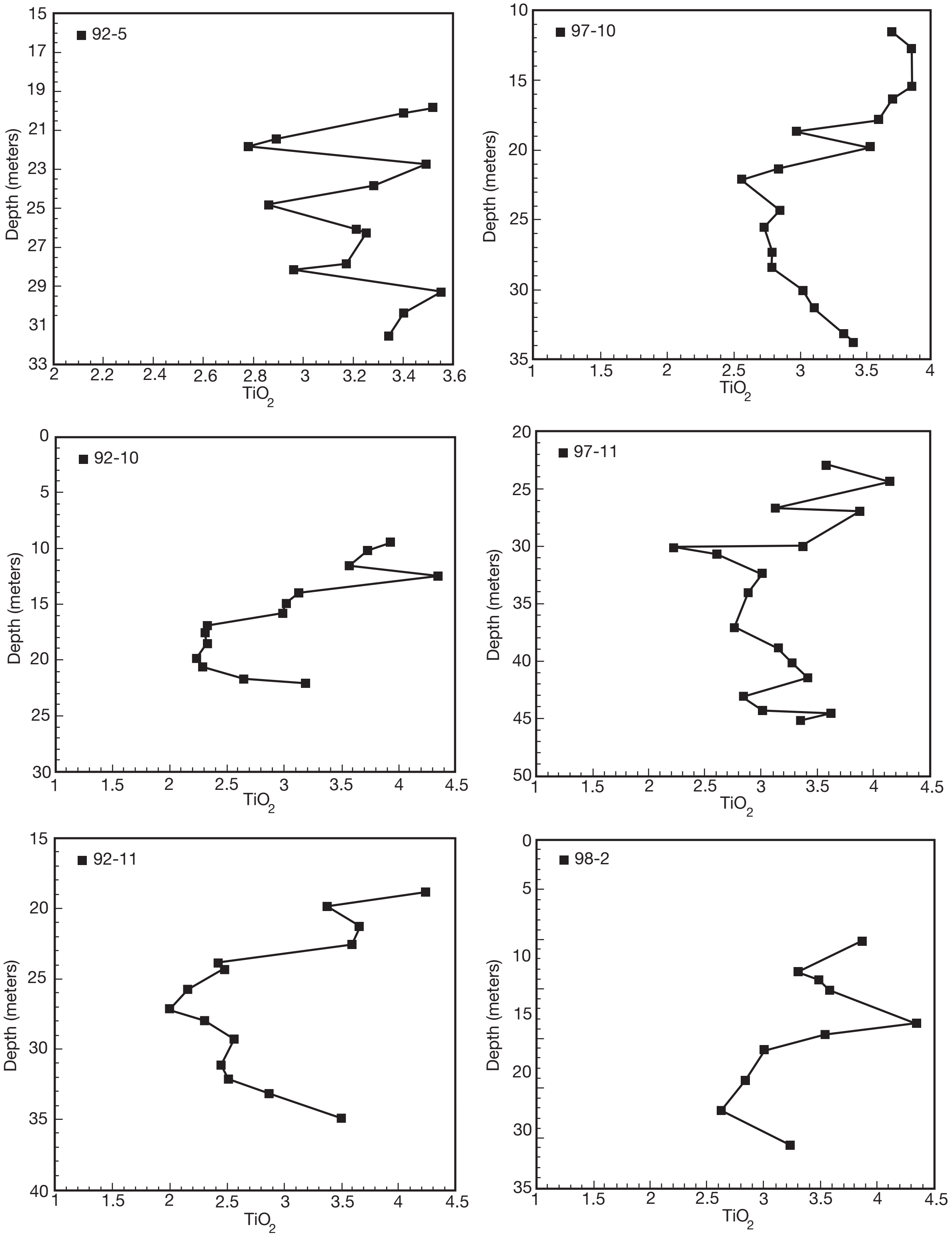

FIGURE 9—The change of TiO_2 concentration of the shallow cores of the Silver City Dome with depth.

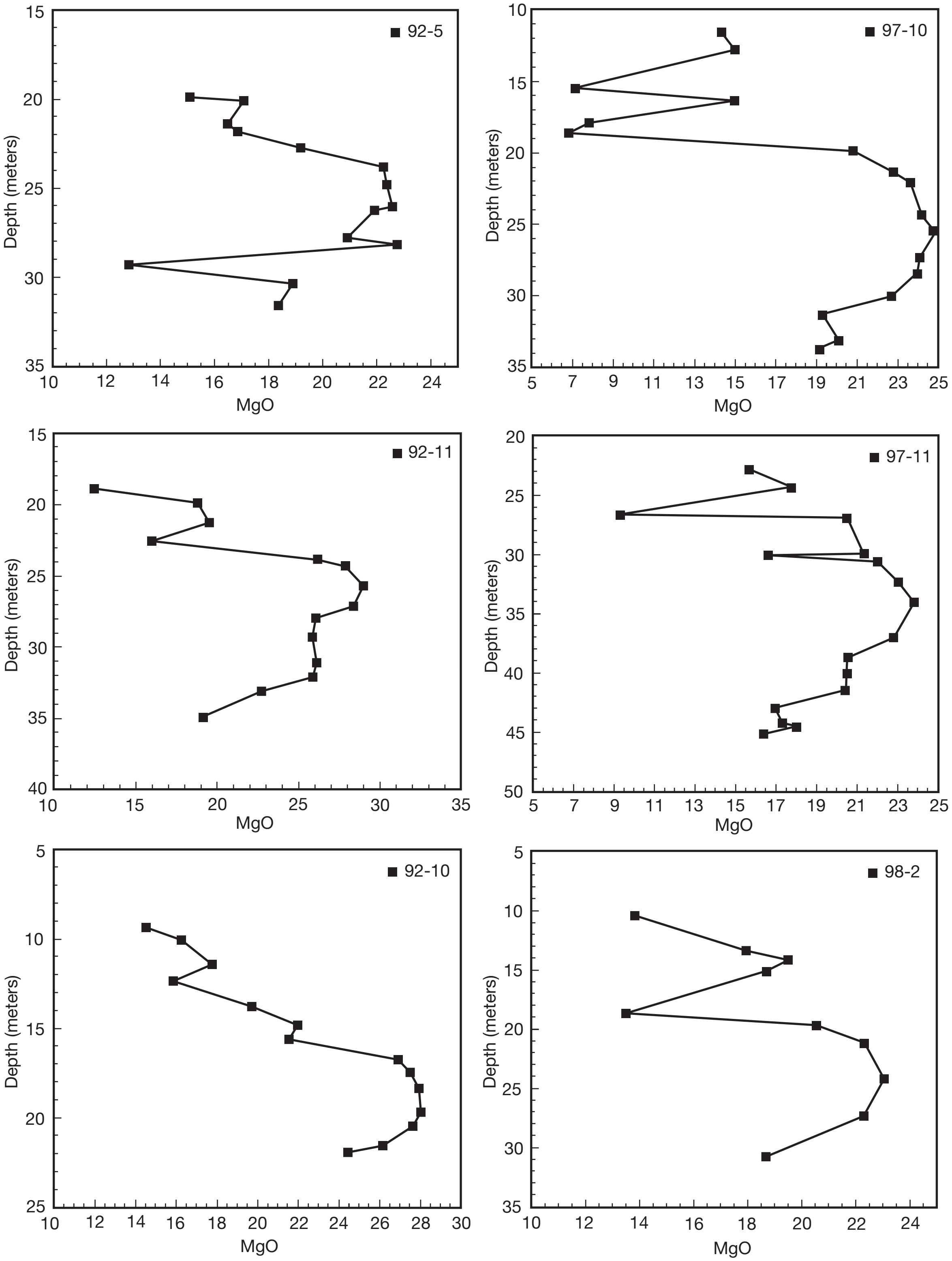

FIGURE 10—The change of MgO concentration of the shallow cores of the Silver City Dome with depth.

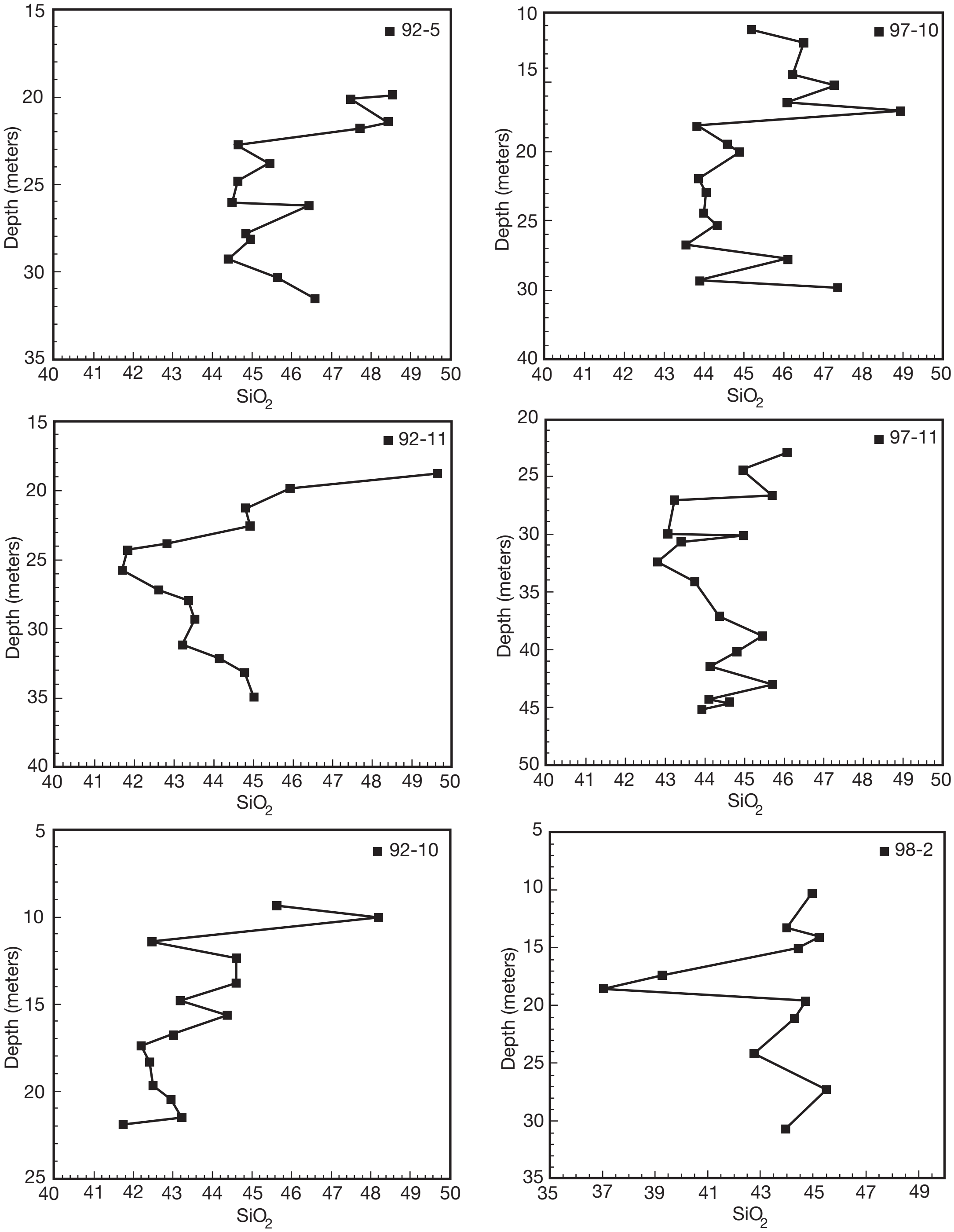

FIGURE 11—The change in SiO$_2$ concentration of the shallow Silver City Dome samples with depth.

Silver City Dome (Foley, 1993; Edgar and Mitchell, 1997; Sato, 1997).

The trace-element contents of the lamproites cannot be quantitatively modeled due to the wide variation in the amount of vein material relative to the harzburgite-lherzolite, to the lack of knowing the concentration of trace elements in the source, and to the lack of appropriate distribution coefficients for lamproite melts relative to minerals. A few comments can tentatively be made about the source of the lamproites from the trace-element data. The high average concentrations of Rb, Ba, Th, U, K, Ta, Nb, and the LREE (fig. 3) suggest that abundant vein material enriched in these elements melted to produce these lamproites (Mitchell and Bergman, 1991). The deeper lamproites at the Silver City Dome tend to have higher average amounts of Rb, Ba, Th, U, K, Ta, Nb, and the LREE than those at the Rose Dome (fig. 8). This suggests that a higher ratio of the vein material to lherzolite-harzburgite melted to form the lamproites at the Silver City Dome than those at Rose Dome consistent with the conclusion based on the SiO$_2$ and MgO contents above. This is not a clear-cut difference as some of the shallower lamproites at the Silver City Dome are lower in some elements (Th, U, Ta, Nb, La) than the lamproites at Rose Dome. There may also be a significant difference in the abundance of these trace elements in the source veins that could explain this difference.

Also these samples contain minimal negative Ta and Nb anomalies in mantle-normalized plots (fig. 8). Negative Ta and

TABLE 5—Averages of lamproites compared to other lamproites.

Woodson County, Kansas					**non-orogenic lamproites**			
	All shallow Silver City-89 samples		**Average of deeper Silver City-21 samples**		**Average of all Rose Dome-29 samples**		**Argylle olivine lamproites-19 samples**	
	Mean	**StDev**	**Mean**	**StDev**	**Mean**	**StDev**	**Mean**	**StDev**
SiO_2	44.58	1.95	46.48	3.78	39.13	1.69	40.04	13.87
TiO_2	3.09	0.55	3.85	1.41	2.63	1.09	3.01	0.48
Al_2O_3	5.64	1.37	7.03	1.57	3.69	0.95	4.78	0.81
Fe_2O_3(total)	7.79	0.50	7.94	1.18	8.81	0.94	8.40	0.86
MnO	0.12	0.02	0.12	0.02	0.14	0.02	0.13	0.06
MgO	20.20	4.78	13.18	3.89	25.30	4.31	21.00	2.25
CaO	3.98	1.54	4.81	1.14	4.94	2.37	5.00	1.90
Na_2O	1.23	0.51	2.04	0.54	0.65	0.41	0.15	0.05
K_2O	5.78	1.85	8.77	1.23	4.23	1.17	3.51	1.46
P_2O_5	1.02	0.73			1.72	0.84	1.05	0.24
LOI	5.23	1.67	4.58	1.67	7.48	2.10		
Total	99.35	0.49	99.87	0.98	99.34	0.34	99.72	0.23
Rb	149	39	234	65	166	39	248	98
Ba	4779	2673	8339	6650	3427	2122	1098	714
Sr	2380	2911	2998	1049	2068	540	835	332
Th	13.1	4.2	20.9	14.7	22.2	8.5	18.0	4.8
Hf	18.9	6.0	33.2	41.7	12.3	4.8	22.3	5.1
Zr	757	260	1141	72	586	162	746	156
Ta	4	1			6	7	12	2
Co	58.9	22.1	46.3	11.6	67.3	12.0	67.9	13.5
Sc	13.8	5.0	20.5	16.2	15.9	6.2	16.1	2.1
Ni	764	305	501	272	1049	383	968	159
Cr	1056	334	844	313	1146	258	1136	145
U	2.6	0.7			4.5	2.0	2.2	0.3
Y	16.3	3.9	32.3	6.7	22.2	7.0	18.0	2.5
Nb	80.8	20.3	115.0	30.1	97.2	57.5	200.1	27.3
La	185	50	273	143	264	92	122	20
Ce	363	117	495	257	520	178	256	43
Pr	40.2	11.0			57.5	19.6		
Nd	133.9	35.7			195.7	67.3	91.9	14.9
Sm	14.9	3.9	20.2	11.8	22.0	7.8	13.3	2.4
Eu	3.7	1.3	4.2	2.7	5.0	1.4	3.1	0.6
Gd	10.18	2.82			15.03	5.31	7.52	1.44
Tb	1.23	0.30	0.77	0.38	1.82	0.64	1.03	0.18
Dy	3.56	0.85			4.96	1.94		
Ho	0.59	0.14			0.79	0.32	0.78	0.15
Er	1.42	0.30			1.97	0.82		
Tm	0.18	0.04			0.23	0.09		
Yb	1.15	0.25	1.22	0.36	1.44	0.49	1.26	0.17
Lu	0.16	0.04	0.23	0.07	0.20	0.08	0.15	0.02
Cu	49	14			77	37	37	15
Li	44	26			19	11		
Zn	69	10			68	18	102	47
Cs	0.44	0.24			1.03	0.26	9.80	5.67
Ga	14.6	2.6			10.9	3.3	7.9	2.3
Ge	1.41	0.60			1.79	0.42		
Pb	38	15			38	8	81	132
V	92	137			51	62	85	26
K_2O/Na_2O	6.00	4.33	4.69	1.84	9.02	5.06	24.41	12.11
$(K_2O+Na_2O)/Al_2O_3$	1.46	0.26	1.85	0.41	1.56	0.37	0.85	0.32
Mg#	0.73	0.05	0.63	0.07	0.75	0.06	0.73	0.03

TABLE 5 continued

	non-orogenic lamproites		**orogenic lamproites**					
	West Kimberley olivine lamproites-26 samples		**Cuddapah lamproites-37 samples**		**El Tale lamproites, Spain-43 samples**		**Spanish lamproites-5 15 samples**	
	Mean	**StDev**	**Mean**	**StDev**	**Mean**	**StDev**	**Mean**	**StDev**
SiO2	44.58	1.11	45.87	2.24	59.37	0.46	54.13	4.78
TiO2	3.09	1.20	3.64	0.79	1.46	0.00	1.44	0.12
Al2O3	5.64	0.56	5.45	1.80	12.46	0.09	10.15	1.63
Fe2O3(total)	7.79	0.66	10.13	1.90	4.97	0.20	5.79	0.96
MnO	0.12	0.01	0.12	0.05	0.04	0.01	0.08	0.03
MgO	20.20	2.94	14.11	0.51	5.67	0.28	9.95	4.15
CaO	3.98	0.65	8.18	1.59	2.58	0.14	5.07	2.80
Na2O	1.23	0.10	0.20	0.22	1.51	0.18	1.61	0.84
K2O	5.78	0.55	2.90	1.37	8.53	0.18	6.34	2.55
P2O5	1.02	0.35	1.06	0.33	1.20	0.02	0.79	0.29
LOI	5.23		7.45	4.02	1.70	0.21		
Total	99.35	0.91	99.11	0.50	99.47	0.05	100.40	0.61
Rb	149	119	135	124	838	12		
Ba	4779	4815	1095	447	1589	3	2058	702
Sr	2380	111	749	157	521	67	896	547
Th	13.1	12.8	16.4	5.2	113.0	1.0		
Hf	18.9		12.8	1.7	20.0	0.8		
Zr	757	237	482	77	765	20	571	358
Ta	4		7.3	1.8	2	1		
Co	58.9	10.1			25.7	0.6	31.2	6.0
Sc	13.8	5	20.3	1.4	17.1	0.9	18.1	3.4
Ni	764	291	599	188	167	5		
Cr	1056	412	786	192	629	45	758	156
U	2.6	2.8	3.8	1.1	17.8	2.7		
Y	16.3	3.9	24.7	5.7	20.0	1.0		
Nb	80.8	60.9	138.4	41.5	37.3	0.6	32.9	10.1
La	185	97	186	67	72	1		
Ce	363	168	368	128	212	15		
Pr	40.2		41.6	14.7				
Nd	133.9		147.7	50.9	128.5	17.7		
Sm	14.9		20.61	5.90	26.0	0.5		
Eu	3.7		5.37	1.43	4.3	0.5		
Gd	10.18		18.93	5.26	14.20	0.28		
Tb	1.23		1.59	0.31	1.85	0.05		
Dy	3.56		6.63	1.00				
Ho	0.59		1.03	0.14				
Er	1.42		2.46	0.45				
Tm	0.18		0.29	0.03	0.42	0.01		
Yb	1.15		1.74	0.22				
Lu	0.16		0.21	0.03	2.19	0.06		
Cu	49	17	59	13	37	1	42	9
Li	44	2					52	14
Zn	69	10	143	91	74	15	83	11
Cs	0.44		12.97	18.35	13.00	2.26		
Ga	14.6	1.3			23.7	0.6		
Ge	1.41							
Pb	38	13	43	45	50	19		
V	92	47	122	34	114	4	104	13
K_2O/Na_2O	6.00	1.91	69.75	69.35	5.73	0.86	5.59	4.30
$(K_2O+Na_2O)/Al_2O_3$	1.46	0.18	0.64	0.23	0.94	0.01	0.94	0.17
Mg#	0.73	0.02	0.71	0.04	0.72	0.03	0.72	0.02

1–from Jaques et al., 1989

2–from Jaques et al., 1984

3–from Chalapathi Rao et al., 2004

4–from Toscani and Salvioli-Mariani, 2000

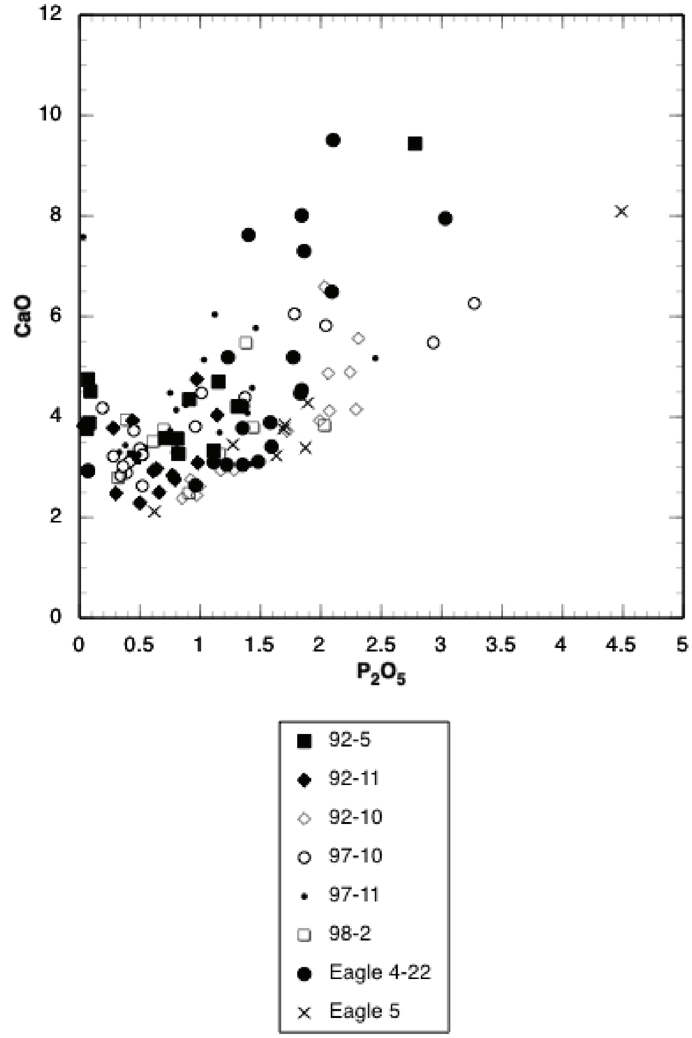

FIGURE 12—The correlation of CaO and P_2O_5 in the shallow Silver City Dome (92-5, 92-11, etc.) and the Rose Dome (Eagle cores).

Nb anomalies are contained in rocks formed by subduction so lamproites with such negative anomalies have been suggested to have source rocks formed by subduction processes (Gibson et al., 1993; Nelson and Davidson, 1993; Wannamaker et al., 2000). Thus, rocks formed by subduction were not likely a significant source during melting to form the southeastern Kansas lamproites. Finally the lack of negative Eu anomalies in the lamproites in chondrite-normalized plots suggests that no feldspar was present in the source during melting or that any significant amount of feldspar crystallized from the melts during fractional crystallization.

Internal Variation within the Sills

The deeper cores at the Silver City Dome were modeled using a settling-floating model of minerals to produce the chemical variation (Cullers et al., 1996). The Ecco Ranch sill was zoned into zones of lower MgO, Fe_2O_3, Co, and Cr concentrations and higher K_2O and Al_2O_3 concentrations. This variation was attributed to decreased ferromagnesian (20% richterite, 27% phlogopite, and 5% diopside removed) and increased sanidine (5.9% added) relative to the estimated average-melt composition.

The Guess sill has less mineralogical-chemical variation than the Ecco Ranch sill except for several small zones that were drastically enriched or depleted in some elements. Mineral accumulation-depletion models did not work so well to explain such variations. Likely H_2O-rich fluids, for, example, may have concentrated Ba, Th, Hf, or Sc in some of the last portions of the magma to cause enrichment of these elements locally in minerals like perovskite, shcherbakovite, and wadeite. There was no evidence of volatile loss to the surrounding sedimentary rocks in the deeper cores.

The thick, shallow sill at the Silver City Dome contains significant mineralogical and chemical variations (Cullers et al., 1985). A flow-differentiation model in which coarser crystals of olivine, diopside, richterite, and phlogopite were concentrated into the interior of the sill explained the elemental variation in this sill. The only elemental variation that could not be explained by this model was Ba, and to a lesser extent, K_2O and Rb. The amount of Ba, and to a lesser extent, K_2O and Rb, were high in the overlying hornfels compared to the unaltered shales. Also Ba concentrations decreased significantly upward in the sill. Thus, Ba and some K_2O and Rb likely moved upward through the sill into the overlying hornfels.

The six shallow sills at the Silver City Dome in this study have many similar fractionation trends as the previously described shallow sill above. For instance, the high MgO, Mg#, Co, and Ni, and the low SiO_2 in the middle compared to the top and bottom of most cores support the flow-differentiation model in which coarser phenocrysts of the ferromagnesian minerals (olivine, richterite, diopside, and phlogopite) concentrate toward the center of the sills.

Differentiation in the deeper sills at Rose Dome is quite different than the shallow sills at the Silver City Dome as many ferromagnesian minerals (olivine, richterite?, diopside?) occur toward the bottom of the sills relative to phlogopite, perovskite, apatite, ilmenite, and wadeite. Also coarser crystals do not appear to concentrate in the center of these sills. Thus, gravity settling and not flow differentiation may again be dominant control on the variation in the deeper sills at Rose Dome.

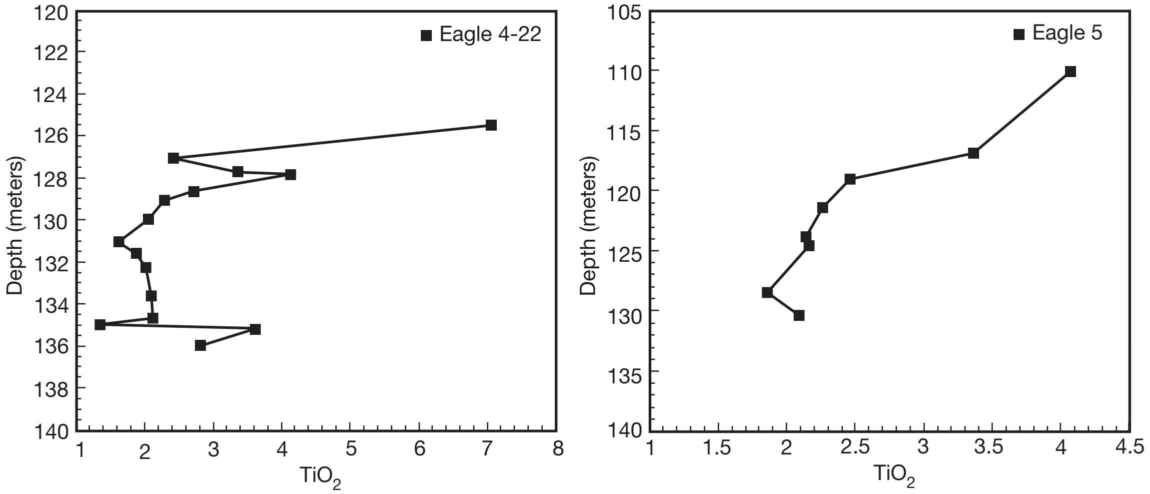

Figure 13—The change of TiO_2 concentration of the shallow cores of the deeper Eagle cores of the Rose Dome with depth.

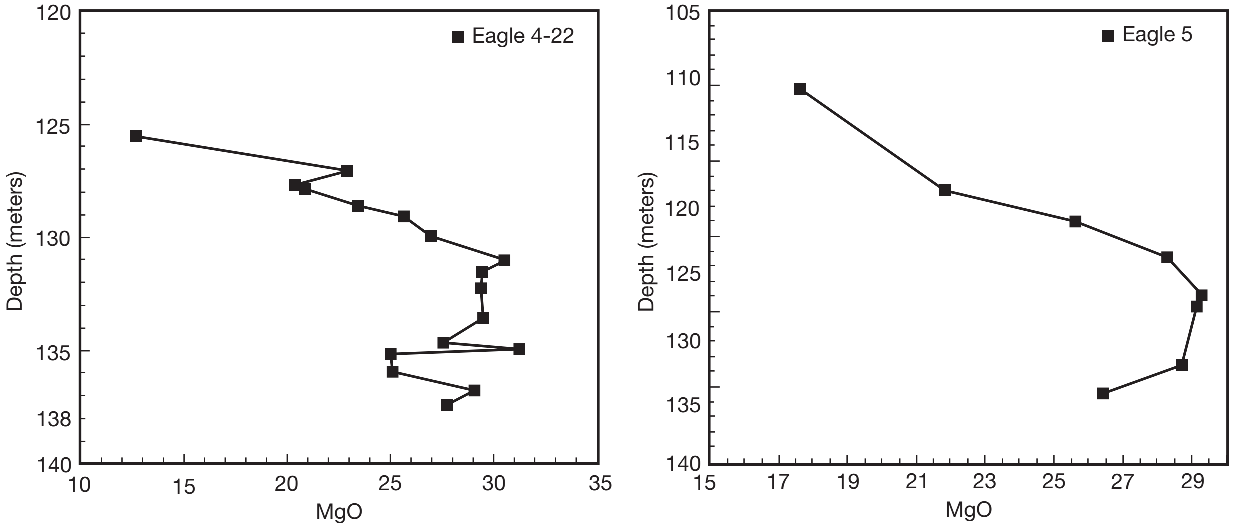

FIGURE 14—The change of MgO concentration of the deeper Eagle cores of the Rose Dome with depth.

References

Altherr, R., Meyer, H. P., Holl, A., Volker, F., Alibert, C., McCulloch, M. T., and Majer, V., 2004, Geochemical and Sr-Nd-Pb isotopic characteristics of Late Cenozoic leucite lamproites from the East European Alpine belt (Macedonia and Yugoslavia): Contributions to Mineralogy and Petrology, v. 147, p. 58–73.

Berendsen, P., 2011, Structural setting and stratigraphy of lamproite occurrences in Woodson and Wilson counties, southeast Kansas, USA: Kansas Geological Survey, Open-file Report 2011-x, 74 p.

Bergman, S. C., 1987, Lamproites and other potassium-rich igneous rocks—a review of their occurrence, mineralogy, and geochemistry; *in*, Alkaline Igneous Rocks, J. G. Fitton and B. G. J. Upton, eds: Geological Society of America, Special Publication, v. 30, p. 103–190.

Chalapathi Rao, N. V., Gibson, S. A., Pyle, D. M., and Dickin, A. P., 2004, Petrogenesis of Proterozoic lamproite and kimberlites from the Cuddapah Basin and Dharwar Craton, southern India: Journal of Petrology, v. 45, p. 907–948.

Coopersmith, H. and Mitchell, R., 1989, Geology and exploration of the Rose lamproite, southeast Kansas, USA; *in*, Kimberlites and Related Rocks—Their Mantle/Crust Setting, Diamonds and Diamond Exploration, A. L. J. Ross, J. Ferguson, D. H. Green, S. Y. O'Reilly, R. V. Danchin, and A. J. A. Janse, eds.: Geological Society of Australia, Special Publication, v. 14, p. 1,179–1,191.

Cullers, R. L., Dorais, M. J., Berendsen, P., and Chaudhuri, S., 1996, The mineralogy and petrology of subsurface lamproites, late Cretaceous age, southeastern Kansas, USA: Lithos, v. 38, p. 185–206.

Cullers, R. L., Ramakrishnan, S., Berendsen, P., and Griffin, T., 1985, Geochemistry and petrogenesis of lamproites, Late Cretaceous age, Woodson County, Kansas, U.S.A.: Geochimica et Cosmochimica Acta, v. 49, p. 1,383–1,402.

Edgar, A. D., and Mitchell, R. H., 1997, Ultra high pressure-temperature melting experiments on an SiO_2-rich lamproite from Smoky Butte, Montana—Derivation of siliceous lamproite magmas from enriched sources deep in the continental mantle: Journal of Petrology, v. 38, p. 457–477.

Foley, S. F., 1992, Vein-plus-wall-rock melting mechanisms in the lithosphere and the origin of potassic alkaline magmas: Lithos, v. 28, p. 435–453.

Foley, S. F., 1993, An experimental study of olivine lamproites—first results from the diamond stability field: Geochimica et Cosmochimica Acta, v. 57, p. 483–489.

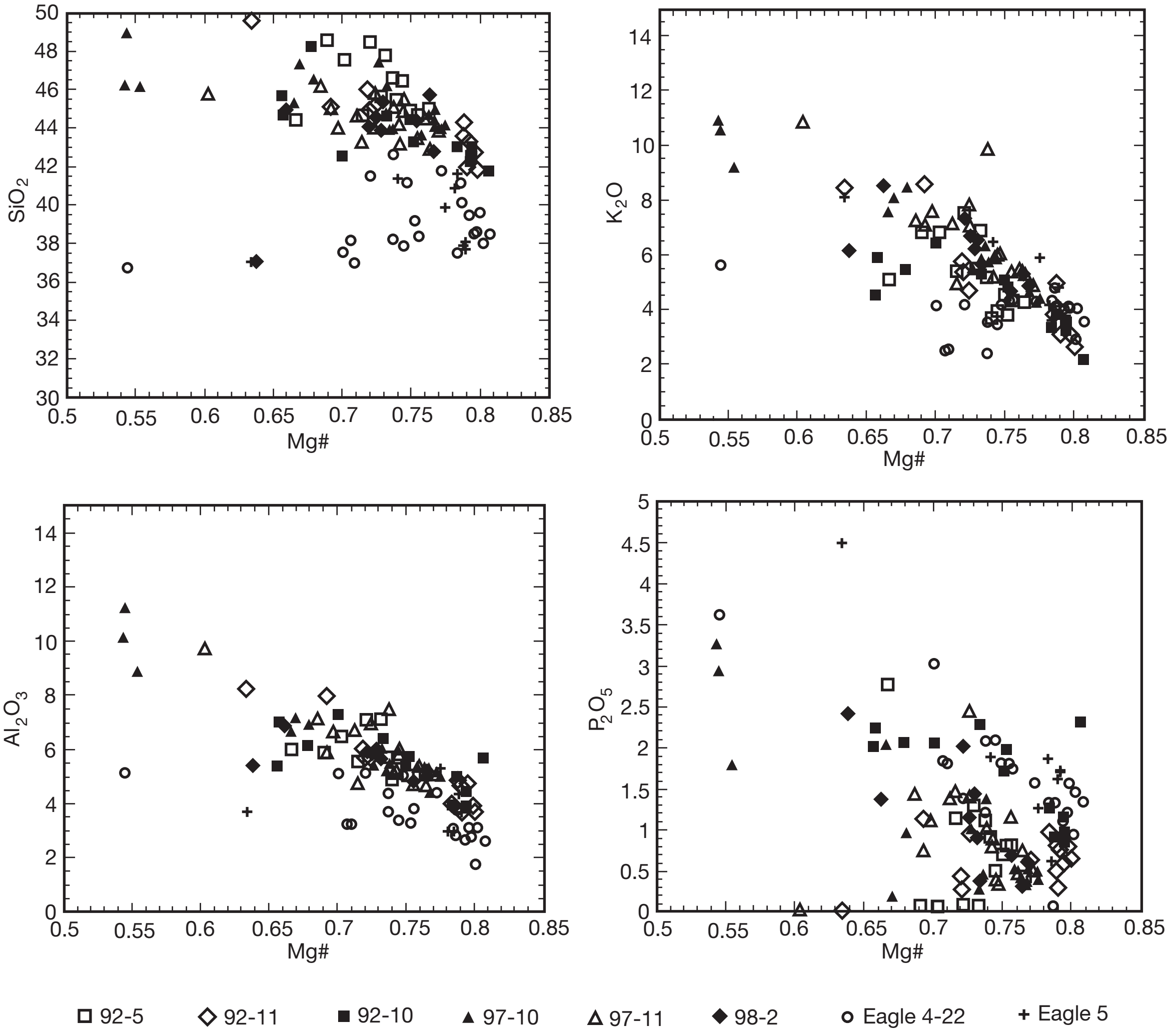

FIGURE 15—The change of SiO_2. Al_2O_3, K_2O, and P_2O_5 with Mg# of the deeper Eagle cores of the Rose Dome and the shallow Silver City Dome.

Foley, S. F., 1994, Geochemische und experimentelle Untersuchungen zur Genese der kalireichen Magmatite: Neus Jahrb. Mineral. Abh., v. 167, p. 1–55.

Foley, S. F., Venturelli, G., Green, D. H., and Toscani, I., 1987, The ultrapotassic rocks—characteristics, classification, and constraints for petrogenetic models: Earth Science Review, v. 24, p. 81–134.

Franks, P., Bickford, M., and Wagner, H. C., 1971, Metamorphism of Precambrian granitic xenoliths in a mica peridotite at Rose Dome, Woodson County, Kansas—Part 2, Petrologic and mineralogic studies: Geological Society of America Bulletin, v. 82, p. 2,869–2,890.

Garbe–Schonberg, C.–D., and McMurtry, G. M., 1994, In-situ micro-analysis of platinum and rare earths in ferromanganese crusts by laser ablation-ICP-MS (LAICPMS): Fresenius' Journal of Analytic Chemistry, v. 350, nos. 4–5, p. 264–271.

Gibson, S. A., Thompson, R. N., P. T. Leat, P. T., Morrison, M. A., Hendry, G. L., Dickin, A. P., and Mitchell, J. G., 1993, Ultrapotassic magmas along the flanks of the Oligocene–Miocene Rio Grande Rift, USA—Monitors of the zone of lithospheric mantle extension and thinning beneath a continental rift: Journal of Petrology, v. 34, p. 187–228.

Govindaraju, K., 1994, 1994 compilation of working values and descriptions for 383 geostandards: Geostandards Newsletter, v. 12, p. 63–118.

Jaques, A. L., Lewis, J. D., and Smith, C. B., 1986, The kimberlites and lamproites of Western Australia: Geological Survey of Western Australia, Bulletin, v. 132, 268 p.

Jaques, A. L., Lewis, J. D., Smith, C. B., Gregory, G. P., Ferguson, J., Chappell, B. W., and McCulloch, M. T., 1984, The diamond-bearing ultrapotassic (lamproitic) rocks of the West Kimberley Region, Western Australia; *in*, Kimberlites I—Kimberlites and Related Rocks, J. Kornprobst, ed.: Amsterdam, Elsevier, v. I, p. 225–254.

Jaques, A. L., Sun, S. S., and Chappell, B. W., 1989, Geochemistry of the Argyle lamproite pipe, Western Australia; *in*, Kimberlites and Related Rocks—Their Composition, Occurrence, Origin, and Emplacement, A. L. J. J. Ross, J. Ferguson, D. H. Green, S. Y. O'Reilly, R. V. Danchin, and A. J. A. Janse, eds.: Geological Society of Australia, Special Publication, v. 14, p. 170–188.

McDonough, W. F., Sun, S.-S., Ringwood, A. E., Jagoutz, E., and Hofmann, A. W., 1992, Potassium, rubidium, and cesium in the earth and moon and the evolution of the mantle of the earth: Geochimica et Cosmochimica Acta, v. 56, p. 1,001–1,012.

Mitchell, R. H., 1985, A review of the mineralogy of lamproites: Transactions of the Geological Society of South Africa, v. 88, p. 411–437.

Mitchell, R. H., 1995, Melting experiments on a sanidine phlogopite lamproite at 4-7 BPa and their bearing on the source of lamproitic magmas: Journal of Petrology, v. 36, p. 1,445–1,474.

Mitchell, R. H., and Bergman, S. C., 1991, Petrology of lamproites: New York, Plenum Press.

Mitchell, R. H., and Edgar, A. D., 2002, Melting experiments on SiO_2-rich lamproites to 6.4 GPa and their bearing on the sources of lamproite magmas: Mineralogy and Petrology, v. 74, p. 115–128.

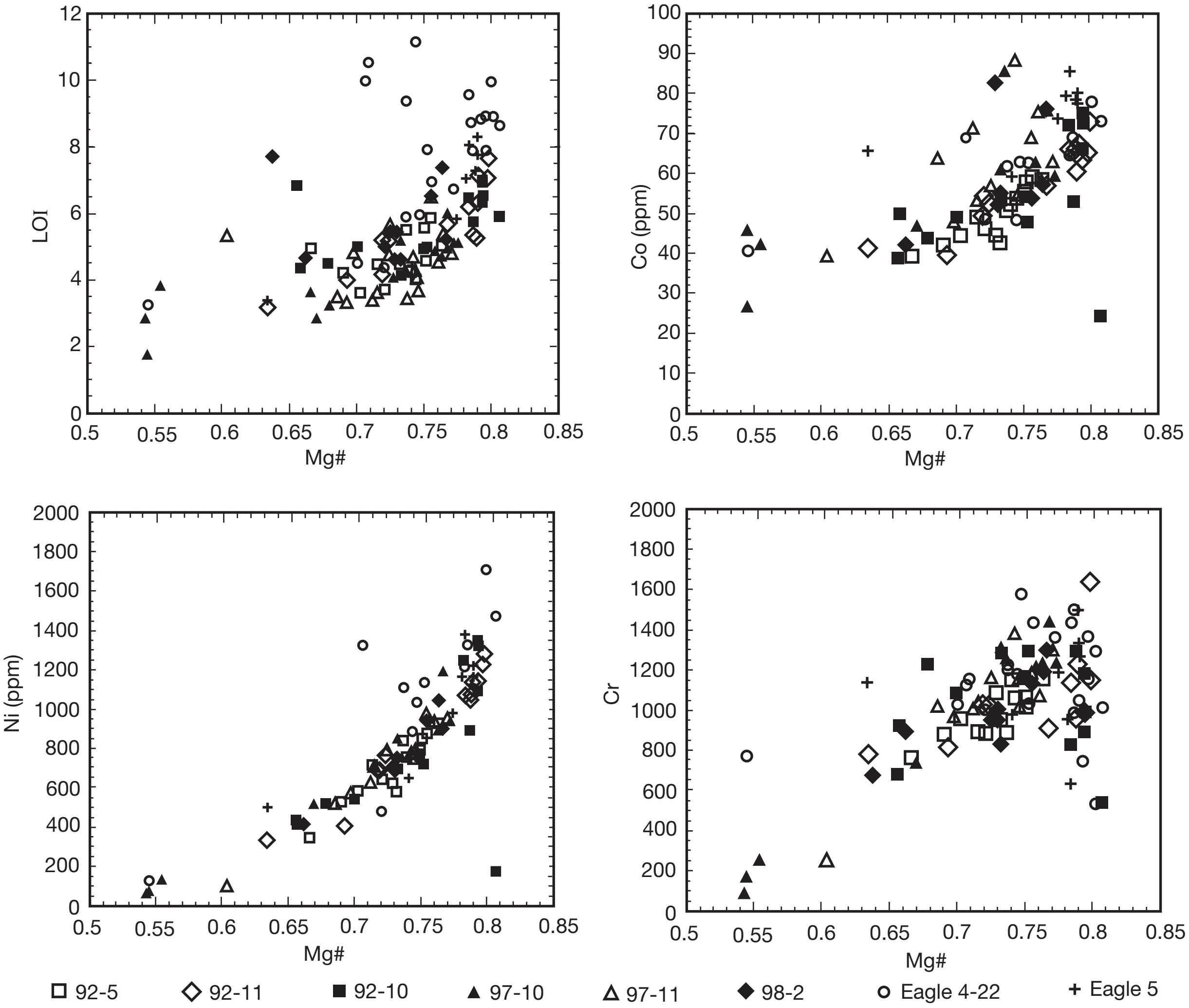

FIGURE 16—The change of LOI, Ni, Co, and Cr with Mg# of the deeper Eagle cores of the Rose Dome and the shallow Silver City Dome.

Nelson, S. T., and Davidson, J. P., 1993, Interactions between mantle-derived magmas and mafic crust, Henry Mountains, Utah: Journal of Geophysical Research, v. 98, p. 1,837–1,852.

Sato, K., 1997, Melting experiments on a synthetic olivine lamproite up to 8 GPa—Implications to its petrogenesis: Journal of Geophysical Research, v. 102, p. 14,751–14,764.

Toscani, L., and Slavioli–Mariani, E., 2000, The lamproite of El Tale (Fortuna, southeast Spain): Chem. Erde, v. 60, p. 96–110.

Wannamaker, P. E., Hulen, J. B., and others, 2000, Early Miocene lamproite from the Colorado Plateau tectonic province, southeastern Utah, USA: Journal of Volcanic and Geothermal Research, v. 96, p. 175–190.